Volume 6 • Issue 3 • June 2012

Editor-in-Chief
Professor Hu, Yu-Chen

INTERNATIONAL JOURNAL OF IMAGE PROCESSING (IJIP)

ISSN : 1985-2304
Publication Frequency: 6 Issues Per Year

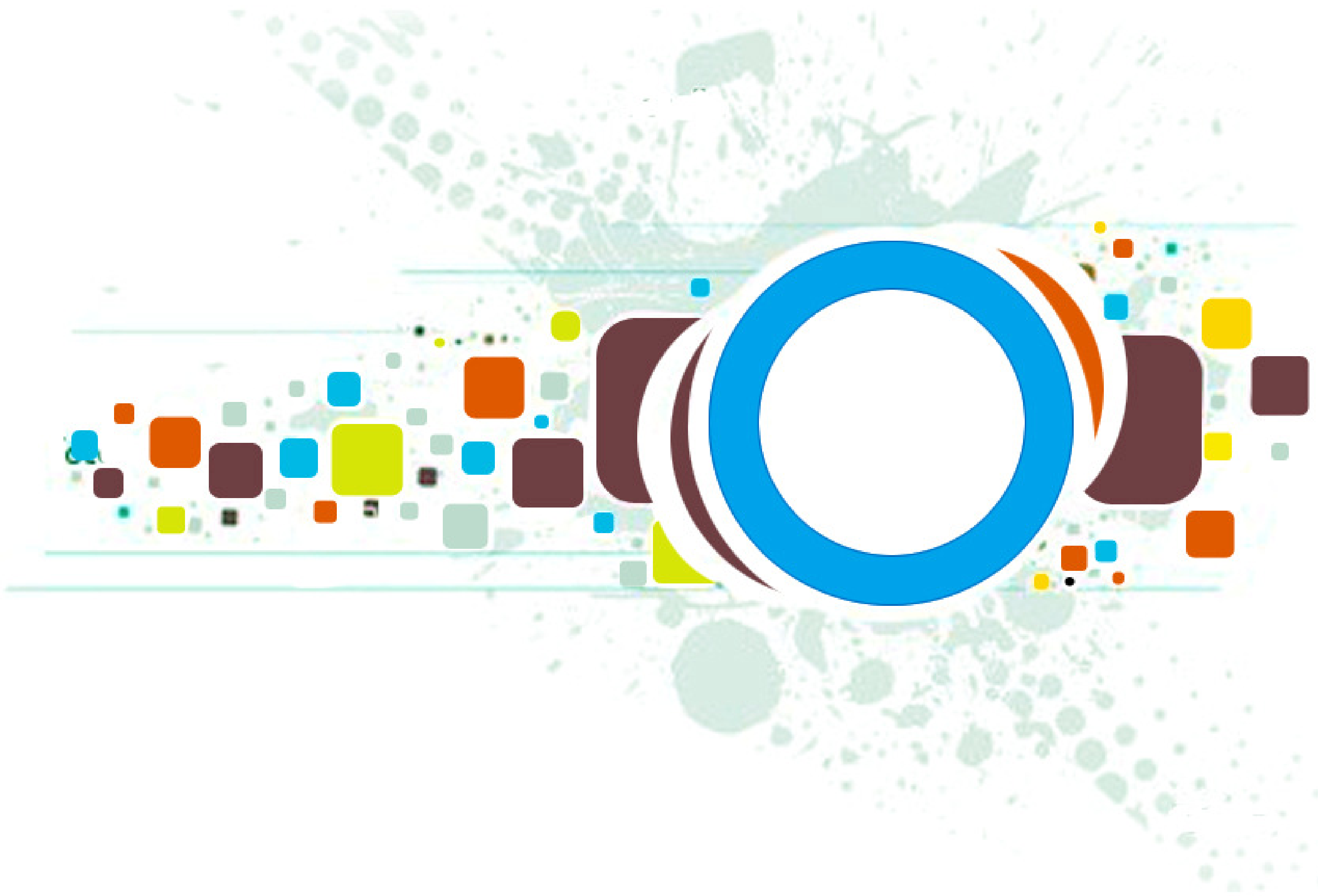

CSC PUBLISHERS
http://www.cscjournals.org

INTERNATIONAL JOURNAL OF IMAGE PROCESSING (IJIP)

VOLUME 6, ISSUE 3, 2012

EDITED BY
DR. NABEEL TAHIR

ISSN (Online): 1985-2304

International Journal of Image Processing (IJIP) is published both in traditional paper form and in Internet. This journal is published at the website http://www.cscjournals.org, maintained by Computer Science Journals (CSC Journals), Malaysia.

IJIP Journal is a part of CSC Publishers
Computer Science Journals
http://www.cscjournals.org

INTERNATIONAL JOURNAL OF IMAGE PROCESSING (IJIP)

Book: Volume 6, Issue 3, June 2012
Publishing Date: 20-06- 2012
ISSN (Online): 1985-2304

IJIP Journal is a part of CSC Publishers
http://www.cscjournals.org

Published in Malaysia

Typesetting: Camera-ready by author, data conversation by CSC Publishing Services – CSC Journals, Malaysia

CSC Publishers, 2012

EDITORIAL PREFACE

The International Journal of Image Processing (IJIP) is an effective medium for interchange of high quality theoretical and applied research in the Image Processing domain from theoretical research to application development. This is the second issue of volume six of IJIP. The Journal is published bi-monthly, with papers being peer reviewed to high international standards. IJIP emphasizes on efficient and effective image technologies, and provides a central for a deeper understanding in the discipline by encouraging the quantitative comparison and performance evaluation of the emerging components of image processing. IJIP comprehensively cover the system, processing and application aspects of image processing. Some of the important topics are architecture of imaging and vision systems, chemical and spectral sensitization, coding and transmission, generation and display, image processing: coding analysis and recognition, photopolymers, visual inspection etc.

The initial efforts helped to shape the editorial policy and to sharpen the focus of the journal. Starting with volume 6, 2012, IJIP appears in more focused issues. Besides normal publications, IJIP intends to organize special issues on more focused topics. Each special issue will have a designated editor (editors) – either member of the editorial board or another recognized specialist in the respective field.

IJIP gives an opportunity to scientists, researchers, engineers and vendors from different disciplines of image processing to share the ideas, identify problems, investigate relevant issues, share common interests, explore new approaches, and initiate possible collaborative research and system development. This journal is helpful for the researchers and R&D engineers, scientists all those persons who are involve in image processing in any shape.

Highly professional scholars give their efforts, valuable time, expertise and motivation to IJIP as Editorial board members. All submissions are evaluated by the International Editorial Board. The International Editorial Board ensures that significant developments in image processing from around the world are reflected in the IJIP publications.

IJIP editors understand that how much it is important for authors and researchers to have their work published with a minimum delay after submission of their papers. They also strongly believe that the direct communication between the editors and authors are important for the welfare, quality and wellbeing of the Journal and its readers. Therefore, all activities from paper submission to paper publication are controlled through electronic systems that include electronic submission, editorial panel and review system that ensures rapid decision with least delays in the publication processes.

To build its international reputation, we are disseminating the publication information through Google Books, Google Scholar, Directory of Open Access Journals (DOAJ), Open J Gate, ScientificCommons, Docstoc and many more. Our International Editors are working on establishing ISI listing and a good impact factor for IJIP. We would like to remind you that the success of our journal depends directly on the number of quality articles submitted for review. Accordingly, we would like to request your participation by submitting quality manuscripts for review and encouraging your colleagues to submit quality manuscripts for review. One of the great benefits we can provide to our prospective authors is the mentoring nature of our review process. IJIP provides authors with high quality, helpful reviews that are shaped to assist authors in improving their manuscripts.

Editorial Board Members
International Journal of Image Processing (IJIP)

TABLE OF CONTENTS

Volume 6, Issue 3, June 2012

Pages

A New Method for Indoor-outdoor Image Classification Using Color Correlated Temperature

A. Nadian Ghomsheh a_nadian@sbu.ac.ir
Electrical and Computer Engineering Department
Shahid Beheshti University
Tehran, 1983963113, Iran

A. Talebpour talebpour@sbu.ac.ir
Electrical and Computer Engineering Department
Shahid Beheshti University
Tehran, 1983963113, Iran

Abstract

In this paper a new method for indoor-outdoor image classification is presented; where the concept of Color Correlated Temperature is used to extract distinguishing features between the two classes. In this process, using Hue color component, each image is segmented into different color channels and color correlated temperature is calculated for each channel. These values are then incorporated to build the image feature vector. Besides color temperature values, the feature vector also holds information about the color formation of the image. In the classification phase, KNN classifier is used to classify images as indoor or outdoor. Two different datasets are used for test purposes; a collection of images gathered from the internet and a second dataset built by frame extraction from different video sequences from one video capturing device. High classification rate, compared to other state of the art methods shows the ability of the proposed method for indoor-outdoor image classification.

Keywords: Indoor-outdoor Image Classification, Color Segmentation, Color Correlated Temperature

1. INTRODUCTION

Scene classification problem is a big challenge in the field of computer vision [1]. With rapid technological advances in digital photography and expanding online storage space available to users, demands for better organization and retrieval of image data base is increasing. Precise indoor-outdoor image classification improves scene classification and allows such processing systems to improve the performance by taking different methods based on the scene class [2]. To classify images as indoor-outdoor, it is common to divide an image into sub-blocks and process each block separately, benefiting from computational ease. Within each image sub-block, different low-level features such as color, texture, and edge information are extracted and used for classification.

Color provides strong information for characterizing landscape senses. Different color spaces have been tested for scene classification. In a pioneer work [3], an image was divided into 4×4 blocks, and Ohta color space [4]was used to construct the required histograms for extracting color information. Using only color information they achieved a classification accuracy of 74.2%. LST color space used by [5] achieved a classification accuracy of 67.6%. [6] used first order statistical features from color histograms, computed in RGB color space, and achieved a classification rate with 65.7% recall and 93.8% precession. [7] compared different features extracted from color histograms. These features include: opponent color chromaticity histogram, color correlogram [8], MPEG-7 color descriptor, colored pattern appearance histogram [9], and layered color indexing [10].Results of this comparison showed that no winner could be selected for all types of images but significant amount of redundancy in histograms can be removed. In [11] mixed channels of RGB, HSV, and Luv color spaces were incorporated to calculate color histograms. First and second order statistical moments of each histogram served as significant features for indoor-outdoor classification. To improve classification accuracy, camera metadata related to capture conditions was used in [12]. In [13], each image was divided into 32×24 sub-blocks and a 2D color histogram in Luv color space along with a composite feature that correlates region color with spatial location derived from H component in HSV color space where used for indoor-outdoor image classification. [14, 15] proposed Color Oriented Histograms (COH) obtained from images divided into 5 blocks. They also used Edge Oriented Histograms (EOH) and combined them together to obtain CEOH as the feature to classify images into indoor-outdoor classes.

Texture and Edge features were also used for indoor-outdoor image classification. [5] extracted texture features obtained from a two-level wavelet decomposition on the L-channel of the LST color space[16]. In [17] each image was segmented via fuzzy C-means clustering and the extracted mean and variance of each segment represented texture features. [18] used variance, coefficient of variation, energy, and entropy to extract texture features for indoor-outdoor classification. Texture orientation was considered in [19]. From the analysis of indoor and outdoor images, and images of synthetic and organic objects, [20] observed that organic objects have a larger amount of small erratic edges due to their fractal nature. The synthetic objects, in comparison, have edges that are straighter, and less erratic.

Although color has shown to be a strong feature for indoor-outdoor image classification, dividing images into different blocks regardless of the information present in each individual image will degrade the classification results, as the mixture of colors in each block would be unpredictable. Another thing that has not gained much attention is the scene illumination where the image was captured in. This is an important aspect since indoor and outdoor illuminations are quite different and incorporating such information can effectively enhance the classification results.

To overcome such limitations when color information is considered for indoor-outdoor image classification, a new method based on the Color Correlated Temperature feature (CCT) is proposed in this paper. As will be shown, the apparent color of an object will change when the scene illumination changes. This feature can be very effective for the aims of this paper, since the illuminants of indoor scenes are much different compared to outdoor scenes. CCT is a way to show the apparent color of an image under different lighting conditions. In this process, each image is divided into different color segments and CCT is found for each segment. These values form the image feature vector, where, other than CCT information, color formation of the image is inherently present in the feature vector. In the classification phase KNN classifier is used for classification [21]. The focus of this paper is on the ability of color information for indoor-outdoor image classification. Edge and texture features can also be added to the image to enhance the classification rate, but this is beyond the scope of this paper.

The reminder of the paper is organized as follows: section 2 reviews the theory of color image formation in order to provide insight to why the concept of CCT can be effective for the aims of this research. In section 3 the proposed method for calculating the temperature vector for an arbitrary image is explained. Section 4 shows the experimental results, and section 5 concludes the paper.

2. REVIEW OF COLOR IMAGE THEORY

A color image is result of light illuminating the scene, the way objects reflect the light hitting their surfaces, and characteristics of the image-capturing device. In the following subsections, first, Dichromatic Reflection Model (DRM) is described and then various light sources are briefly looked at to show differences among them. This explanation shows why the concept of CCT can be utilized for indoor-outdoor image classification.

2.1 Dichromatic Reflection Model

A scene captured by a color camera can be modeled by spectral integration. This is often described by DRM. Light striking a surface of non-homogeneous materials passes through air and contacts the surface of the material. Due to difference in mediums index of refraction, some of the light will reflect from the surface of the material which is called surface reflectance (Ls). The light that penetrates into the body of the material is absorbed by the colorant, transmitted through the material, or will re-emit from the entering surface. This component is called the body reflectance (Lb). [22]. The total light (L), reflected from an object is the sum of surface and body reflectance, and can be formulized as;

$$L(\lambda,\Omega) = L_s(\lambda,\Omega) + L_b(\lambda,\Omega) \tag{1}$$

where, λ is the wavelength of the incident light and Ω the photometric angle that includes the viewing angle e, the phase angle g, and the illumination direction angle i (fig.1). Ls and Lb are both dependent on the relative spectral power distribution (SPD), defined by Cs and Cb, and a geometric scaling factor ms and mb which can be formulized by;

$$L_s(\lambda,\Omega) = m_s(\Omega)C_s(\lambda) \tag{2}$$

$$L_b(\lambda,\Omega) = m_b(\Omega)C_b(\lambda) \tag{3}$$

Cs and Cb are also both product of the incident light spectrum (E), and the material's spectral surface reflectance (ρS) and body reflectance (ρB), defined by;

$$C_s(\lambda) = E_s(\lambda)\rho_s(\lambda) \tag{4}$$

$$C_b(\lambda) = E_b(\lambda)\rho_b(\lambda) \tag{5}$$

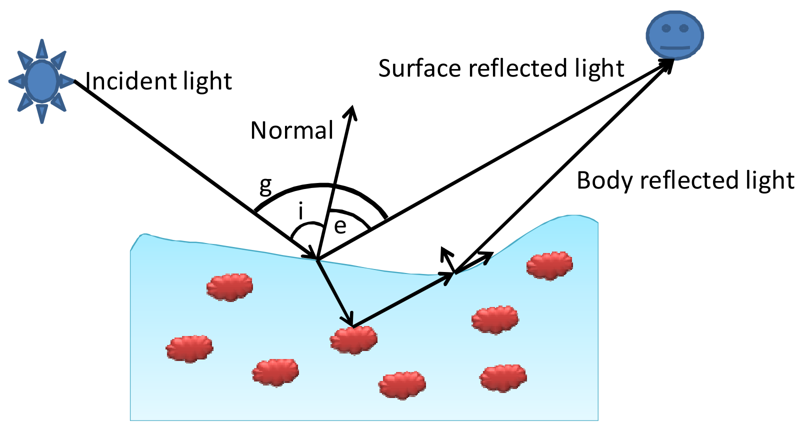

FIGURE 1: DRM model, showing surface reflectance and body reflectance from surface of an object.

By inspecting equations, (2) to (5) it can be observed that the light that enters into the camera is dependent on the power spectrum of the light source; therefore, for the same object different apparent color is perceived under different illuminations. Due to this fact, it can be implied that different groups of illuminants give an object different perceived colors. The less within class variance among a group of light sources and the more between class variance among different groups of light sources indicate a better distinguishing feature for indoor outdoor image classification when scene illumination is considered. In the next subsection different light sources are reviewed to how different classes of light sources differ from each other.

2.2- Light Sources

The color of a light source is defined by its spectral composition. The spectral composition of a light source may be described by the CCT. A spectrum with a low CCT has a maximum in the radiant power distribution at long wavelengths, which gives the material a reddish appearance, e.g. sunlight during sunset. A light source with a high CCT has a maximum in the radiant power distribution at short wavelengths and gives the material a bluish appearance, e.g., special fluorescent lamps [23]. Fig 2-a shows three fluorescent lamp SPDs compared with a halogen bulb, and Fig 2-b shows SPD of daylight in various hours of day. Comparison between these two types shows how the spectrums of fluorescents lamps follow the same pattern and how they are different with respect to the halogen lamp.

Fig. 2-c shows three diverse light spectrums; Blackbody radiator, a fluorescent lamp, and daylight all having a CCT of 6200 K. It can be seen that the daylight spectrum is close to the Blackbody spectrum whereas the fluorescent lamp spectrum deviates significantly from the blackbody spectrum.172 light sources measured in [24] showed that illuminant chromaticity

falls on a long thin band in the chromaticity plane which is very close to the Planckian locus of Blackbody radiators

By reviewing the SPDs of various light sources it can be implied that the same group of light sources show the same pattern in their relative radiant power when compared to other groups. This distinguishing feature makes it possible to classify a scene based on scene illuminant; which in this paper is incorporated for indoor-outdoor image classification.

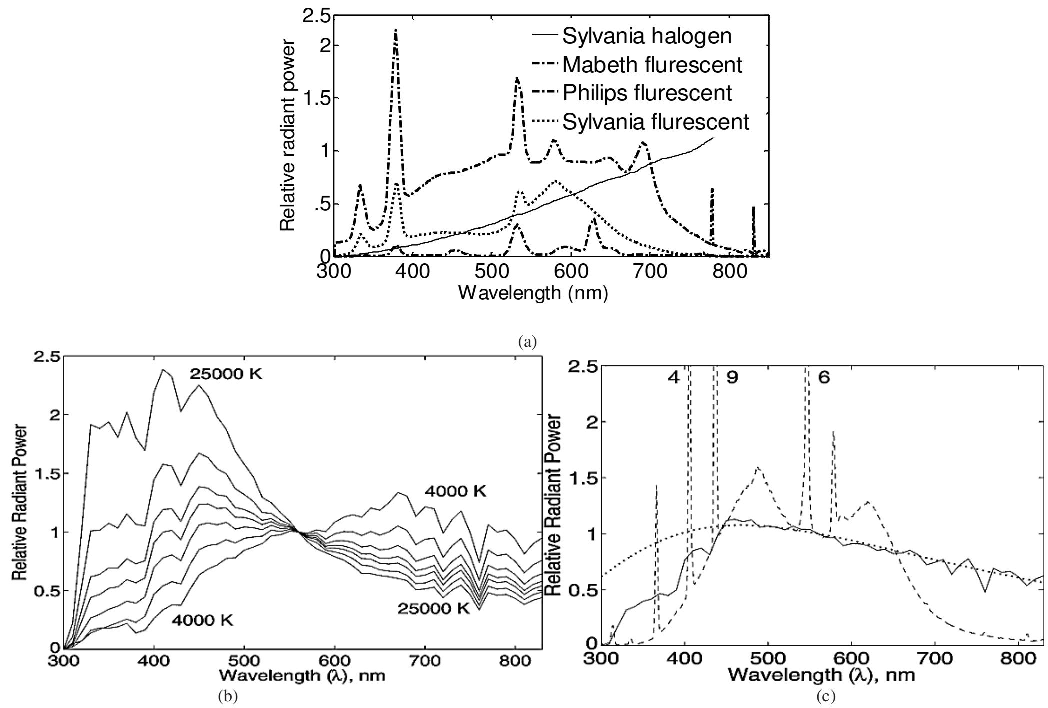

FIGURE 2: Different light sources with their SPDs. (a) SPDs for three different fluorescent lamps compared to SPD of halogen bulb [23]. (b) Daylight SPDs at different hours of day, normalized at 560nm. (c) Spectra of different light sources all with a CCT of 6200K and normalized at λ = 560 nm [24].

3. PROPOSED METHOD

Review of color image formation showed that the color of an image captured by the camera is result of the reflected light from the surface of objects as a sum of body and surface reflectance (eq. 1). Surface reflectance has same properties of the incident light and it is a significant feature for detecting the light source illuminating the scene. Body reflectance on the other hand most closely resembles the color of the material taking into account the spectra of the incident light; which in this paper is used as a metric to classify images as indoor and outdoor. Different steps of the proposed algorithm are shown in fig. 3.

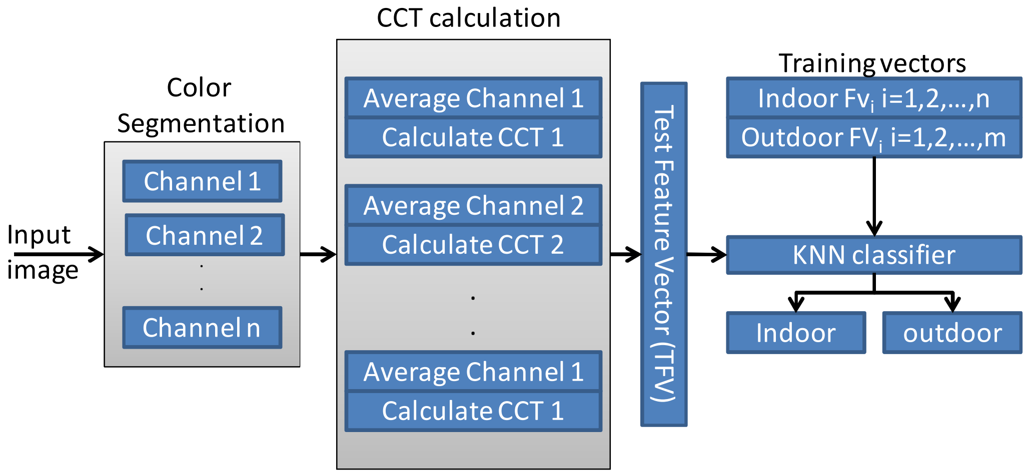

FIGURE 3: Block Diagram of the proposed method for indoor-outdoor classification

In the first step, color segmentation is performed and the image is partitioned into N color channels (each color segment is thought of an independent color channel). Next CCT is calculated for each channel, and the feature vector obtained is used for indoor-outdoor image classification. Finally a KNN classifier is used to partition images into two classes of indoor and outdoor. Each step of the algorithm is next explained in detail.

3.1 Color Segmentation

Many color spaces have been used for color segmentation. HSV is nonlinear color spaces and a cylindrical-coordinate representation of points in RGB color model. The nonlinear property of this color space makes it possible to segment colors in one color component independent of other components which is an advantage over linear color spaces [25]. This is color space is used here to segment images into desired number of segments; where each segment is called a "color channel". HSV is obtained from RGB space by:

$$h = \begin{cases} 0 & \text{if } \max = \min \\ \left(60^\circ \times \frac{g-b}{\max - \min}\right) \bmod 360^\circ & \text{if } \max = r \\ 60^\circ \times \frac{b-r}{\max - \min} + 120^\circ & \text{if } \max = g \\ 60^\circ \times \frac{r-g}{\max - \min} + 240^\circ & \text{if } \max = b \end{cases} \tag{6}$$

$$s = \begin{cases} 0 & \text{if } \max = 0 \\ 1 - \min/\max & \text{otherwise} \end{cases} \tag{7}$$

$$v = \max \tag{8}$$

here max and min are the respective maximum and minimum values of r, g, and b, the RGB color components for each pixel in the image.

The following steps show how each image is converted to its corresponding color channels (*Ch*).For an input image with color components: Red, Green, and Blue:

1) Convert image from RGB color space to HSV
2) Quantize H component to 2^n where $n=1,2,\ldots,N$
3) Find a mask that determines each color channel (*ch*):

$$\begin{aligned} &\text{if } H(x,y) = n \quad && mask_n(x,y) = 1 \\ &\text{else} && mask_n(x,y) = 0 \end{aligned}$$

4) Each *Ch* is then obtained by:

$$Ch_n = [(mask_n.red), (msk_n.Green), (mask_n.Blue)]$$

where "." Represent point-by-point multiplication of matrixes. After dividing each image into the respective color channels, CCT for each available channel has to be calculated.

3.2 Calculating CCT

A few algorithms have been introduced to estimate temperature of a digital image for scene classification or finding scene illumination[26, 27]. Different purpose of the previous algorithms makes them impractical for the aim of this paper.

Planckian, or blackbody locus can by calculated by colorimetrically integrating the Planck function at many different temperatures, with each temperature specifying a unique pair of chromaticity coordinates on the locus [28]. Inversely if one has the Planckian locus, then CCT can be calculated for every chromaticity coordinate. To find the CCT for each color channel it is necessary to find a chromaticity value to represent each color channel. The algorithm proposed for calculation CCT for each color channel has the following steps:

1) From V component of HSV color space, discard dark pixels that their value is smaller than 10% of maximum range of V for each *ch*.
2) Take average of the remaining pixels in RGB color space to discard surface reflectance through the iterative process.
3) Find the CCT of the color channel using the average chromaticity value.

From the DRM model it will be straight forward that dark pixels in the image do not hold information about the scene luminance since they are either not illuminated, or the reflected light from their surface does not enter the camera. In steps 2, pixels, which their values hold information mainly about surface reflectance, are discarded through an iterative process. In this process instead of just discarding bright points, the algorithm discards pixels with respect to luminance of other pixels. Using this average value, the CCT of each color channel is the calculated.

3.2.1 Calculating Average Chromaticity of L_b

The aim of averaging each channel is to discard pixels that have been exposed to direct light, or where the reflection from object's surface is in line with camera lenses. The value of such pixels may vary with respect to the surface reflectance and lighting condition. The flow chart to implement the proposed algorithm is shown in Fig. 4.

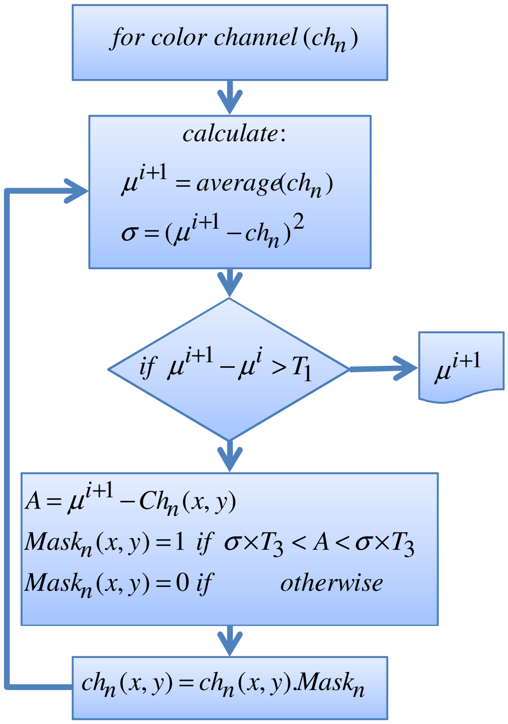

FIGURE 4: Different steps of color segmentation process

In this algorithm, *Ch(x,y)* is pixel value at position *(x,y)* in Ch_n, *M* is the mask that discards the unwanted information. "." is the inner product. σ is variance, and μ is the mean value of the remaining pixels in iteration *i*. *T1*, *T2*, and *T3* are the thresholds that have to be determined. The convergence of this algorithm is guaranteed since in worth case only one pixel of the image will be left unchanged and the calculated μ for that pixel will stay constant. Therefore, thresholds *T1*, *T2*, and *T3* can be chosen arbitrary. However, to find a good set of thresholds they are found by training them on 40 training images. To do so it is desired to find triple $T=(T_1,T_2,T_3)$ that for each color channel the best average point is obtained. This point is defined as "the point where the average values that is most frequently occurred". Let each $Ch_{i,n,C}$ be all the training color channels:

$$ch_{i,n,C} = \begin{bmatrix} ch_{1,1,1} & \cdots & ch_{1,n,1} \\ \vdots & \begin{bmatrix} ch_{1,1,2} & \cdots & ch_{1,n,2} \\ \vdots & & \\ ch_{i,1,2} & \begin{bmatrix} ch_{1,1,3} & \cdots & ch_{1,n,3} \\ \vdots & \ddots & \vdots \\ ch_{i,1,3} & \cdots & ch_{i,n,3} \end{bmatrix} & \end{bmatrix} & \\ ch_{i,1,} & & \end{bmatrix} \tag{9}$$

where *i (i=1,2,…,I)* is the number of image samples, *n (n= 1,2,…,N)* is the number of color channel in each image, and *C (C=1,2,3)* shows Red, Green, and Blue components. Also let T_1, T_2, and T_3 be vectors:

$$T_1 = [1.05, 1.1, ..., 1.3]$$
$$T_2 = [1.1, 1.2, ..., 1.5]$$
$$T_3 = [1, 2, ..., 5],$$

which can take the form:

$$T(\alpha) = \left\{ (T_1^{\,1} T_2^{\,1} T_3^{\,1}), (T_1^{\,1} T_2^{\,1} T_3^{\,2}), ..., (T_1^{\,6} T_2^{\,6} T_3^{\,5}) \right\} \tag{10}$$

where α=*1,2,…,180*. Set *T*(α) consists of all threshold combinations that have to be checked in order to find the best choice of thresholds, $\boldsymbol{T^{opt}}$. For each sample *Ch*, the average value of the channel in the respective color component is calculated for *T*(α), and stored in the average vector ***Avg***:

$$\boldsymbol{Avg}(\alpha) = [Avg(T(1)), Avg(T(2)),..., Avg(T(180))] \quad (11)$$

Next, the histogram of ***Avg*** with ten bin resolution is calculated (Fig. 5). The most frequent bin is considered as the acceptable average values of the *Ch* defined by Avg_{max}. Set T^{opt} shows the thresholds that yield Avg_{max} for a certain *Ch*, and is defined as:

$$T^{opt} = \underset{T(\alpha)}{\arg\max}\, \boldsymbol{Avg}(T(\alpha)) \quad (12)$$

By calculating T^{opt} for all color channels a set $T^{opt}(t)$, t=1,2,…,960 is achieved which can be written as:

$$T^{obt}(t) = \left\{ \underset{t_{red}=1:320}{T^{opt}{}_{red}}, \underset{t_{green}=321:640}{T^{opt}{}_{Green}}, \underset{t_{blue}=641:960}{T^{opt}{}_{blue}} \right\} \quad (13)$$

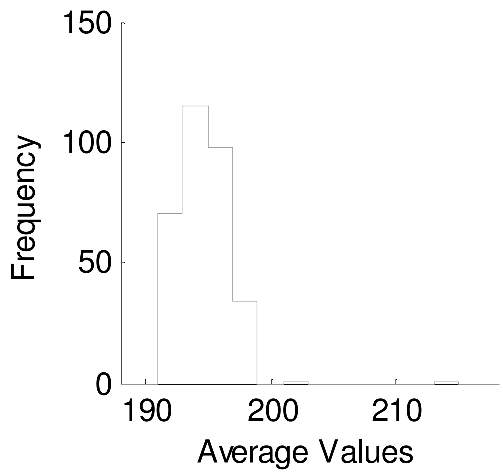

FIGURE 5: Finding different T that yield Avgmax

From this set it is possible to find the optimum thresholds for each color component, for example for the red channel $T^{opt,red}$, can be written as:

$$T^{obt,red} = \underset{t_{red}}{\arg\max}\, T^{opt}{}_{red}(t)` \quad (14)$$

$T^{obt,green}$ and $T^{opt,blue}$ are calculated in the same way as (14), and from them all the trained thresholds are obtained as:

$$\boldsymbol{T^{obt}} = \begin{bmatrix} T_1^{obt,red} & T_1^{obt,green} & T_1^{obt,blue} \\ T_2^{obt,red} & T_2^{obt,green} & T_2^{obt,blue} \\ T_3^{obt,red} & T_3^{obt,green} & T_3^{obt,blue} \end{bmatrix} \quad (15)$$

After calculating the average chromaticity value μ, it is possible to find the CCT of each Ch_n.

3.2.2 Calculating CCT For The Average Chromaticity

To calculate the CCT of a chromaticity value $\mu(x,y)$, it is transformed into Luv color space [25], where pixel μ is represented by coordinates (u,v). Fig 6 shows the Luv chromaticity plane with the plankian locus showing various Color temperatures, the perpendicular lines on the locus are iso-temperature lines.

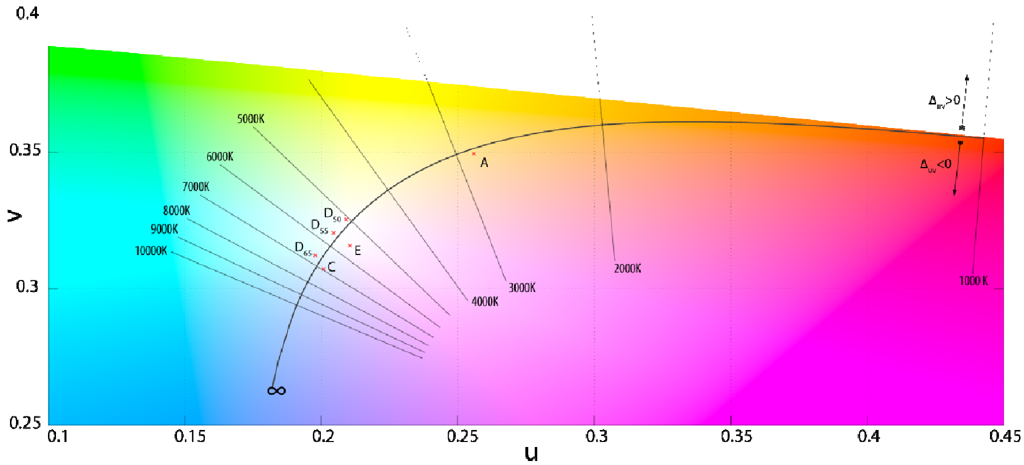

FIGURE 6: Luv chromaticity plane with the plankian locus.

By utilizing iso-temperature line CCT can be found by interpolation from look-up tables and charts. The most famous such method is Robertson's [29] (Fig 7). In this method CCT of a chromaticity value T_c, can be found by calculating:

$$\frac{1}{T_c} = \frac{1}{T_1} + \frac{\theta_1}{\theta_1 + \theta_2}\left(\frac{1}{T_i} - \frac{1}{T_{i+1}}\right) \tag{16}$$

where, θ is the angle between two isotherms. T_i and T_{i+1} are the color temperatures of the look-up isotherms and i is chosen such that $T_i<T_c<T_{i+1}$ (fig 7). If the isotherms are tight enough, it can assumed that, $(\theta_1/\theta_2)\approx(\sin\theta_1/\sin\theta_2)$, leading to:

$$\frac{1}{T_c} = \frac{1}{T_1} + \frac{d_i}{d_i - d_{i+1}}\left(\frac{1}{T_i} - \frac{1}{T_{i+1}}\right) \tag{17}$$

d_i is distance of the test point to the *i'th* isotherm given by:

$$d_i = \frac{(v_c - v_i) - m_i(u_c - u_i)}{\sqrt{1 + m_i^2}} \tag{18}$$

where, (u_i,v_i) is the chromaticity coordinates of the *i'th* isotherm on the Planckian locus and m_i is the isotherm's slope. Since it is perpendicular to the locus, it follows that $m_i=-1/l_i$ where l_i is the slope of the locus at (u_i,v_i). Upon calculation of CCT for all color channels, the feature vector *fv* containing the respective CCT for each color channel is obtained:

$$fv = [CCT_1, CCT_2, ..., CCT_N] \tag{19}$$

where, N is the number of color channels in each image. This vector can now be used for classification. In the classification phase, KNN classifier is used for classification. K is a user-defined constant, and the test feature vectors are classified by assigning the label which is most frequent among the K training samples nearest to that test point.

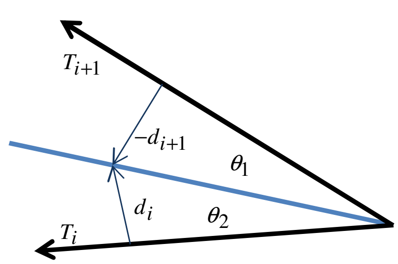

FIGURE 7: Robertson method for finding CCT of a chromaticity value.

4. EXPERIMENTAL RESULTS

To assess the performance of the proposed method, some tests are conducted on two sets of indoor and outdoor images. First a collection 800 images gathered from the internet named DB1 and a second dataset selected by extracting 800 frames from several video clips captured by a Sony HD handy cam (DB2).

Using DB2 it is possible to denote that camera effects are the same for all images; hence the classification ability of the proposed method is evaluated regardless of camera calibrations. A total of 40 clips captured in outdoors, and 25 different clips captured indoor were used to make DB2. The clips were captured at 29.97 frames per second and data were stored in RGB color space with 8bit resolution for each color channel. Fig 8 shows some sample indoor and outdoor frames. To show the difference between normal averaging and the averaging process introduced in this paper where the effect of surface reflectance is eliminated fig 9 is utilized.

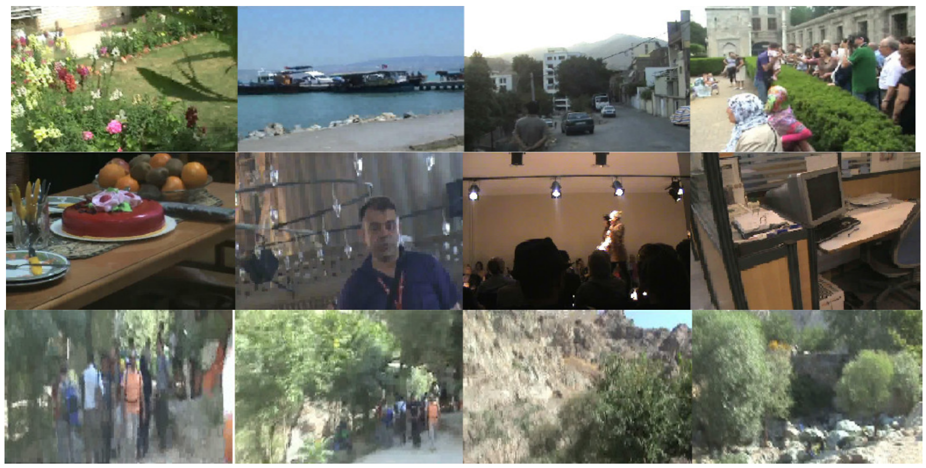

FIGURE 8: Top and middle rows: 4 indoor and outdoor and Bottom row: 4 consecutive outdoor frames

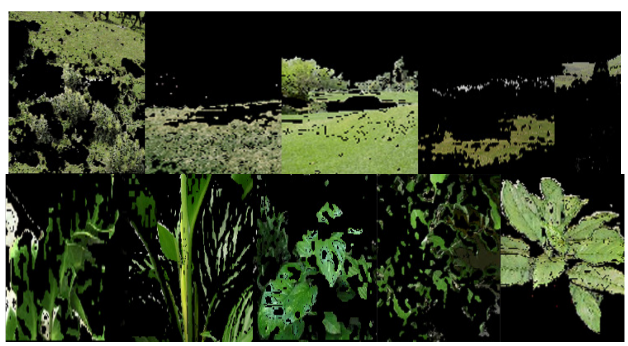

(a)

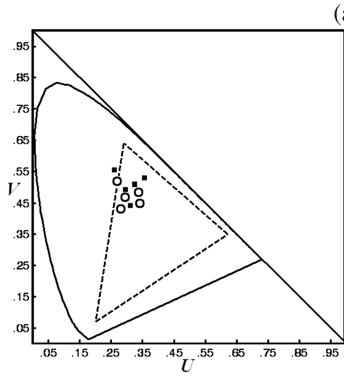

(b)

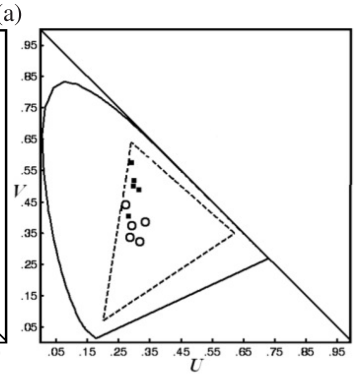

(c)

FIGURE 9: An example of the proposed algorithm for averaging color channels. a) Green channels of pictures taken in outdoor (top row) and at indoor situations (bottom row). (b) Normal averaging of the pixels. (c) Averaging pixels by the proposed algorithm.

Fig 9.a shows ten green color channels from five outdoor and five indoor scenes. For each color channel the corresponding average chromaticity value in the *uv* plane is shown. Outdoor images are shown with circles and indoor images are shown with black squares. As it can be seen when the effect of surface reflectance is obscured, the indoor and outdoor images are significantly separable. To calculate the average points T^{opt} was trained. The histogram of average values obtained for channel $Ch_{1,1,1}$ (as an example) are shown in fig10. Based on the histograms calculated for all different channels, the matrix $\boldsymbol{T^{opt}}$ was obtained as:

$$T^{opt} = \begin{bmatrix} 2 & 1 & 1 \\ 1.1 & 1.2 & 1.1 \\ 1.4 & 1.4 & 1.3 \end{bmatrix}$$

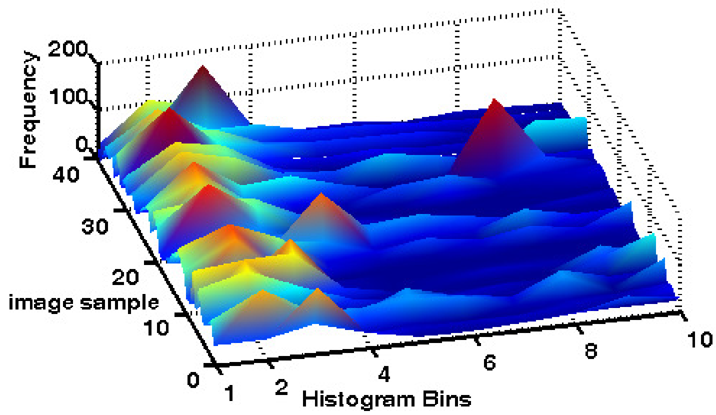

FIGURE 10: Average values of the $Ch_{1,1,1}$ component on the database

		N=4	N=8	N=12	N=16	N=18
K=15	indoor	73.5	90.5	88	85.5	83.2
	outdoor	51	69.2	80.5	89.5	82.4
K=20	indoor	78	86.5	92	87.5	88.1
	outdoor	63.5	74	80.5	89	82.2
K=30	indoor	70	85.5	90	87	87.1
	outdoor	52	72	80	87.5	77.2

TABLE 1: Results of classification on DB1

After finding the *fv* for an image, KNN classifier is used for classification. Table1 shows the result of image classification for different N (number of color channels) and K (number of neighbors in KNN classifier). From this table it can be seen N=16 yields the best result when considering both indoor and outdoor detection rates. Furthermore when K=20 is chosen, 87.5% indoor and 89% outdoor images are correctly classified. Table 2 shows the classification results on DB2. In this experiment, the results also show that choosing 16 channels for classification achieves higher classification rates. The overall comparisons on DB1 and DB2 show that results only differ by a small percentage. This shows that the method is robust for classification of images taken under unknown camera calibration and image compression.

		N=4	N=8	N=12	N=16	N=18
K=15	indoor	77	92.5	91.5	87.5	90.5
	outdoor	54	72	82.5	90	78.5
K=20	indoor	81.5	88.5	90.5	90	85.2
	outdoor	63.5	86	84.5	89.5	86.5
K=30	indoor	74	87.5	88.5	88.5	84.5
	outdoor	57	74.5	82.5	89.5	83.7

TABLE 2: Results of classification on DB2

To observe the results based on accuracy of classification and to find the K which yields the best results, fig. 11 shows the accuracy of each experiment. Based on this figure it can be seen that when DB1 and DB2 with N=16 and K=20 are chosen best classification rates with 88.25% and 89.75% in accuracy are obtained.

In Most cases, it can be seen that indoor images have been detected with more accuracy. This because the outdoor image are exposed to more diverse lighting conditions since the spectrum of sunlight is changing during daytime and also reflections from the sea, clouds and the ground makes the spectrum of the reflected light more complex.

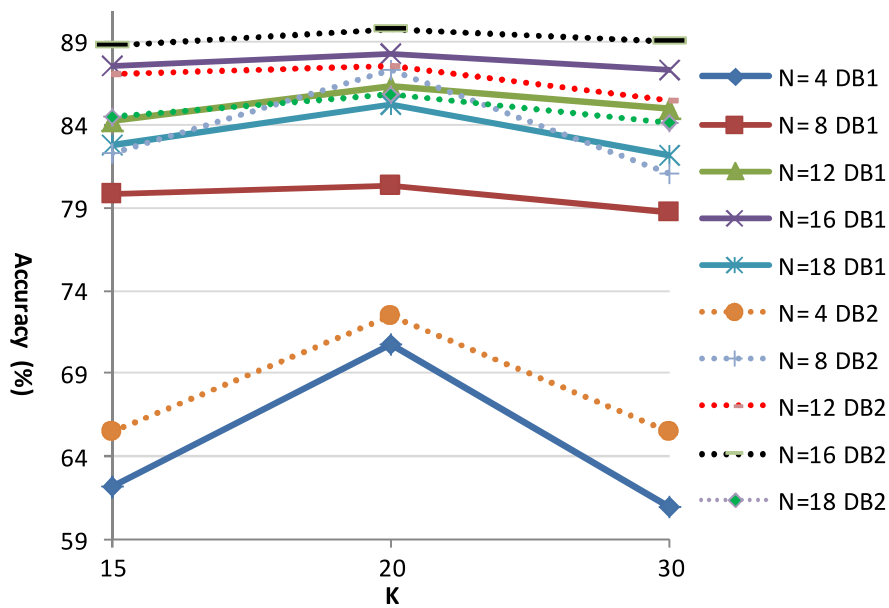

FIGURE 11: Accuracy of the all test cases

To evaluate classification accuracy of the proposed method, two color features: Color Oriented Histograms (COH) and the Ohta color space used in [15] and [3] respectively are extracted and tested on images in DB1. Table 3 shows the result of this comparison. These features are extracted as explained in the original document.

		CCT	COH	Ohta
K=15	Indoor	85.5	94	85.5
	Outdoor	89.5	68.5	70.25
	Accuracy	**87.5**	**81.25**	**78.75**
K=20	Indoor	87.5	95	84
	Outdoor	89	69.5	70
	Accuracy	**88.25**	**82.25**	**77**
K=25	Indoor	87	96.5	86
	Outdoor	87.5	68	68.5
	Accuracy	**87.25**	**82.25**	**77.25**

TABLE 3: Comparison of different methods

From the results of this table, it is clear that the proposed method outperforms the state of the art methods at least by 5%. The indoor classification rate using COH is in most cases more significant in comparison to the classification rate using CCT, but outdoor classification using COH shows quite low detection rates. Ohta color space shows not to be a preferable color space for indoor-outdoor image classification. To further investigate the robustness of the proposed method, in another experiment the result of indoor-outdoor classification is tested when the JPEG Compression Ratio (CR) is changed for image in DB1[30].

		CR=2	CR=3	CR=5	CR=10
CCT	Indoor	86	87.5	77	74.5
	Outdoor	80	76	73	67
	Accuracy	**83**	**81.75**	**75**	**70.75**
COH	Indoor	88	79.5	76	72.5
	Outdoor	62.5	60	53	54.5
	Accuracy	**75.25**	**69.75**	**64.5**	**63.5**
Ohta	Indoor	71	73.5	69.5	63
	Outdoor	69.3	67	61	54.5
	Accuracy	**70.15**	**70.25**	**65.25**	**58.75**

TABLE 4:. Effect of JPEG compression classification results

Table 4 summarizes the result of indoor-outdoor image classification for different compression rates on DB1. From this table it can be seen that the CCT of the image is less affected when CR=2 and 3 but as CR is increased the results for all methods start to degrade. For CR=10 classification accuracy based on CCT feature is still higher than 70% while for two other tested approached , they are decreased to less than 65%. This result shows the robustness of the proposed method against changes in compression changes applied to digital images.

5. CONCLUSIONS

In this paper, a new method based on image CCT was proposed for indoor-outdoor image classification. Images were first segmented into different color channels and based on the proposed algorithm CCT of each color channels was calculated. These CCTs formed the feature vector which was fed to a KNN classifier to classify images as indoor or outdoor. Tests were conducted on two datasets collected from the internet and video frames extracted from 40 different video clips. The classification results showed that incorporating CCT information yields high classification accuracy of 88.25% on DB1 and 89.75% on DB2. The result of classification on DB1 showed 5% improvement compared to other state of the art methods. In addition, the method was tested against changes in the JPEG compression rate applied to images where the method showed to be more robust compared to other methods. High classification rate and robustness of the presented method makes it highly applicable for the application of indoor-outdoor image classification.

6. REFERENCES

[1] Angadi, S.A. and M.M. Kodabagi, *A Texture Based Methodology for Text Region Extraction from Low Resolution Natural Scene Images.* International Journal of Image Processing, 2009. **3**(5): p. 229-245.

[2] Bianco, S., et al., *Improving Color Constancy Using Indoor–Outdoor Image Classification.* IEEE transaction on Image Processing, 2008. **17**(12): p. 2381-2392.

[3] Szummer, M. and R.W. Picard, *Indoor-outdoor image classification*, in *IEEE Workshop on Content-Based Access of Image and Video Database*. 1998: Bombay, India. p. 42-51.

[4] Ohta, Y.I., T. Kanade, and T. Sakai, *Color information for region segmentation.* Computer Graphics and Image Processing, 1980. **13**(3): p. 222-241.

[5] Serrano, N., A. Savakis, and J. Luo, *A computationally efficient approach to indoor/outdoor scene classification*, in *International Conference on Pattern Recognition*. 2002: QC, Canada, . p. 146-149.

[6] Miene, A., et al., *Automatic shot boundary detection and classification of indoor and outdoor scenes*, in *Information Technology, 11th Text Retrieval Conference*. 2003, Citeseer. p. 615-620.

[7] Qiu, G., X. Feng, and J. Fang, *Compressing histogram representations for automatic colour photo categorization.* Pattern Recognition, 2004. **37**(11): p. 2177-2193.

[8] Huang, J., et al., *Image indexing using color correlograms.* International Journal of Computer Vision, 2001: p. 245–268.

[9] Qiu, G., *Indexing chromatic and achromatic patterns for content-based colour image retrieval.* Pattern Recognition, 2002. **35**(8): p. 1675-1686.

[10] Qiu, G. and K.M. Lam, *Spectrally layered color indexing.* Lecture Notes in Computer Science, 2002. **2384**: p. 100-107.

[11] Collier, J. and A. Ramirez-Serrano, *Environment Classification for Indoor/Outdoor Robotic Mapping*, in *Canadian Conference on Computer and Robot Vision*. 2009, IEEE. p. 276-283.

[12] Boutell, M. and J. Luo, *Bayesian Fusion of Camera Metadata Cues in Semantic Scene Classification*, in *Computer Vision and Pattern Recognition (CVPR)*. 2004: Washington, D.C. p. 623-630.

[13] Tao, L., Y.H. Kim, and Y.T. Kim, *An efficient neural network based indoor-outdoor scene classification algorithm*, in *International Conference on Consumer Electronics*. 2010: Las Vegas, NV p. 317-318.

[14] Vailaya, A., et al., *Image classification for content-based indexing.* IEEE Transactions on Image Processing, 2001. **10**(1): p. 117-130.

[15] Kim, W., J. Park, and C. Kim, *A Novel Method for Efficient Indoor–Outdoor Image Classification.* Signal Processing Systems, 2010. **61**(3): p. 1-8.

[16] Daubechies, I., *Ten Lectures on Wavlets*. 1992, Philadelphia: SIAM Publications.

[17] Gupta, L., et al., *Indoor versus outdoor scene classification using probabilistic neural network* Eurasip Journal on Advances in Signal Processing, 2007. **1**: p. 123-133.

[18] Tolambiya, A., S. Venkatraman, and P.K. Kalra, *Content-based image classification with wavelet relevance vector machines.* Soft Computing, 2010. **14**(2): p. 129-136.

[19] Hu, G.H., J.J. Bu, and C. Chen, *A novel Bayesian framework for indoor-outdoor image classification*, in *International Conference on Machine Learning and Cybernetics* 2003: Xian. p. 3028-3032

[20] Payne, A. and S. Singh, *Indoor vs. outdoor scene classification in digital photographs.* Pattern Recognition, 2005. **38**(10): p. 1533-1545.

[21] Songbo, T., *An effective refinement strategy for KNN text classifier.* Expert Systems with Application, 2006. **30**(2): p. 290-298.

[22] Shafer, S.A., *Using color to separate reflection components.* Color Research and Application, 1985. **10**(4): p. 210.

[23] Ebner, M., *Color constancy*. 2007, West Sussex: Wily.

[24] Finlayson, G., G. Schaefer, and S. Surface, *Single surface colour constancy*, in *7th Color Imaging Conference: Color Science, Systems, and Applications*. 1999: Scottsdale, USA. p. 106-113.

[25] Cheng, H.D., et al., *color image segmentation: advances and prospects.* Pattern Recognition, 2001. **34**(12): p. 2259-2281.

[26] WNUKOWICZ, K. and W. SKARBEK, *Colour temperature estimation algorithm for digital images - properties and convergence.* OPTO-ELECTRONICS REVIEW, 2003. **11**(3): p. 193-196.

[27] Lee, H., et al., *One-dimensional conversion of color temperature in perceived illumination.* Consumer Electronics, IEEE Transactions on, 2001. **47**(3): p. 340-346.

[28] Javier, H., J. Romero, and L.R. Lee, *Calculating correlated color temperatures across the entire gamut of daylight and skylight chromaticities.* Applied Optis, 1999. **38**(27): p. 5703-5709.

[29] Robertson, A. and R. Alan, *computation of Correlated Color Temperature abd Distribution Temperature.* Color Research and Application, 1968. **58**(11): p. 1528-1535.

[30] Yang, E. and L. Wang, *Joint optimization of run-length coding, Huffman coding, and quantization table with complete baseline JPEG decoder compatibility.* Image Processing, IEEE Transactions on, 2009. **18**(1): p. 63-74.

Effect of Similarity Measures for CBIR Using Bins Approach

Dr. H. B Kekre *hbkekre@yahoo.com*
Professor,Department of Computer Engineering
NMIMS University,
Mumbai, Vileparle 056, India

Kavita Sonawane *kavitavinaysonawane@gmail.com*
Ph .D Research Scholar
NMIMS University,
Mumbai, Vileparle 056, India

Abstract

This paper elaborates on the selection of suitable similarity measure for content based image retrieval. It contains the analysis done after the application of similarity measure named Minkowski Distance from order first to fifth. It also explains the effective use of similarity measure named correlation distance in the form of angle 'cosθ' between two vectors. Feature vector database prepared for this experimentation is based on extraction of first four moments into 27 bins formed by partitioning the equalized histogram of R, G and B planes of image into three parts. This generates the feature vector of dimension 27. Image database used in this work includes 2000 BMP images from 20 different classes. Three feature vector databases of four moments namely Mean, Standard deviation, Skewness and Kurtosis are prepared for three color intensities (R, G and B) separately. Then system enters in the second phase of comparing the query image and database images which makes of set of similarity measures mentioned above. Results obtained using all distance measures are then evaluated using three parameters PRCP, LSRR and Longest String. Results obtained are then refined and narrowed by combining the three different results of three different colors R, G and B using criterion 3. Analysis of these results with respect to similarity measures describes the effectiveness of lower orders of Minkowski distance as compared to higher orders. Use of Correlation distance also proved its best for these CBIR results.

Keywords: Equalized Histogram, Minkowski Distance, Cosine Correlation Distance, Moments, LSRR, Longest String, PRCP.

1. INTRODUCTION

Research work in the field of CBIR systems is growing in various directions for various different stages of CBIR like types of feature vectors, types of feature extraction techniques, representation of feature vectors, application of similarity measures, performance evaluation parameters etc[1][2][3][4][5][6]. Many approaches are being invented and designed in frequency domain like application of various transforms over entire image, or blocks of images or row column vector of images, Fourier descriptors or various other ways using transforms are designed to extract and represent the image feature[7][8][9][10][11][12]. Similarly many methods are being design and implemented in the spatial domain too. This includes use of image histograms, color coherence vectors, vector quantization based techniques and many other spatial features extraction methods for CBIR [13][14][15][16][17]. In our work we have prepared the feature vector databases using spatial properties of image in the form statistical parameters i.e. moments namely Mean, Standard deviation, Skewness and Kurtosis. These moments are extracted into 27 bins formed by partitioning the equalized histograms of R, G and B planes of image into 3 parts.[18][19][20]. The core part of all the CBIR systems is calculating the distance between the query image and database images which has great impact on the behavior of the CBIR system as it actually decides the set of images to be retrieved in final retrieval set. Various similarity measures are available can be used for CBIR [21][22][23][24]. Most commonly used similarity measure we have seen in the literature survey of CBIR is Euclidean distance. Here we have used Minkowski distance from order first to fifth where we found that performance of the system goes on improving with decrease in the order (from 5 to 1) of Minkowski distance; one more similarity measure we have used in this work is Cosine Correlation distance [25][26][27][28], which has also proved its best after Minkowski order one. Performance of CBIR's various methods in both frequency and spatial domain will be evaluated using various parameters like precision, recall, LSRR (Length of String to Retrieve all Relevant) and various others [29][30][31][32][33]. In this paper we are using three parameters PRCP, LSRR and 'Longest String' to evaluate the performance of our system for all the similarity measures used and for all types of feature vectors for three colors R, G and B. We found scope to narrate and combine these results obtained separately for three feature vector databases based on three colors. This refinement is achieved using criterion designed to combine results of three colors which selects the image in final retrieval set even though it is being retrieved in results set of only one of these three colors [11[12].

2. ALGORITHMIC VIEW WITH IMPLEMENTATION DETAILS

2.1 Bins Formation by Partitioning the Equlaized Histogram of R, G, B Planes

i. First we have separated the image into R, G and B Planes and calculated the equalized histogram for each plane as shown below.

ii. These histograms are then partitioned into three parts with id '0', '1' and '2'. This partitioning generates the two threshold for the intensities distributed across x – axis of histogram for each plane. We have named these threshold or partition boundaries as GL1 and GL2 as shown in Figure 2.

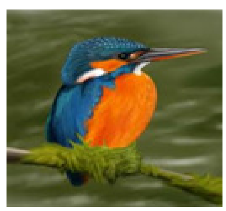

FIGURE 1: Query Image: Kingfisher

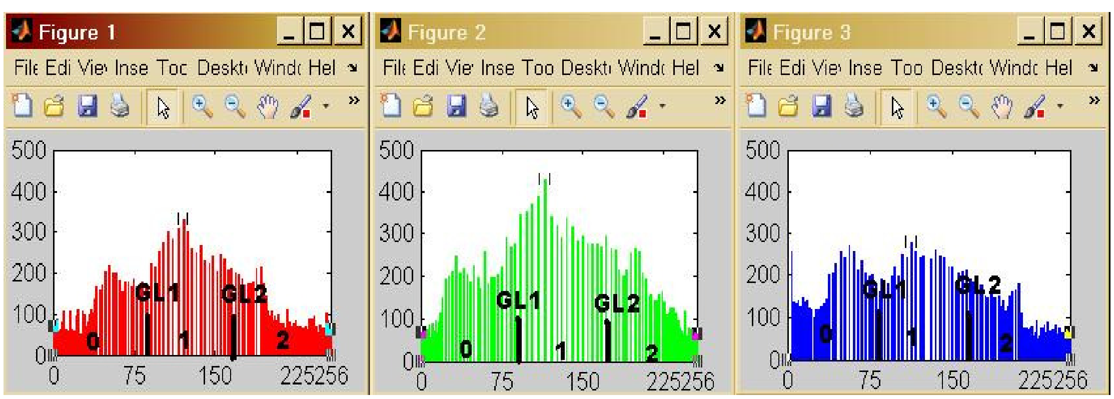

FIGURE 2: Equalized Histograms of R, G and B Planes With Three partitions '0', '1' and '2'.

iii. Determination of Bin address: To determine the destination for the pixel under process of extracting feature vector we have to check its R, G and B intensities where they fall, in which partition of the respective equalized histogram either '0','1' or '2' and then this way 3 digit flag is assigned to that pixel itself its destination bin address. Like this we have obtained 000 to 222 total 27 bin addresses by dividing the histogram into 3 parts.

2.2 Statistical Information Stored in 27 Bins: Mean, Standard Deviation, Skewness and Kurtosis

Basically these bins obtained are having the count of pixels falling in particular range. Further these bins are used to hold the statistical information in the form of first four moments for each color separately. These moments are calculated for the pixel intensities coming into each bin using the following Equations 1 to 4 respectively.

Mean	$\overline{R} = \frac{1}{N}\sum_{i=1}^{N} R_i$	**(1)**	**Skew**	$R_{SK} = \frac{1}{N}\sqrt[3]{\sum_{i=1}^{N}(R_i - \overline{R})^3}$	**(3)**
Standard deviation	$R_{SD} = \frac{1}{N}\sqrt{\sum_{i=1}^{N}\left(R - \overline{R}\right)^2}$	**(2)**	**Kurtosis**	$R_{KU} = \frac{1}{N}\sqrt[4]{\sum_{i=1}^{N}(R_i - \overline{R})^4}$	**(4)**
Where $\overline{R}$ is Bin_Mean_R in eq. 1, 2, 3 and 4.					

These bins are directed to hold the absolute values of central moments and likewise we could obtained 4 moments x 3 colors =12 feature vector databases, where each feature vector is consist of 27 components. Following Figure 3 shows the bins of R, G, B colors for Mean parameter. Sample 27 Bins of R, G and B Colors for Kingfisher image shown in Figure 1.

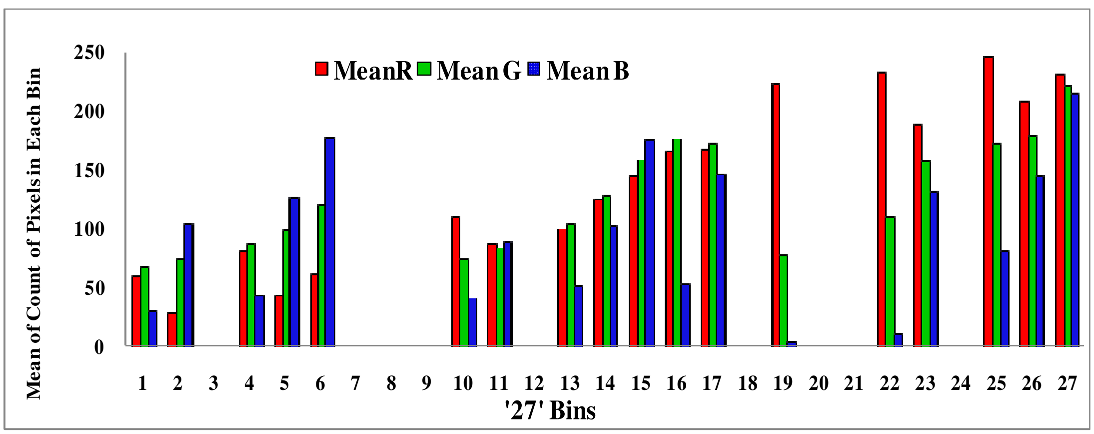

FIGURE 3: 27 Bins of R, G and B Colors for MEAN Parameter.

In above Figure 3 we can observe that Bin number 3, 7, 8, 9, 12, 18, 20, 21 and 24 are empty because the count of pixels falling in those bins is zero in this image.

2.3 Application of Similarity Measures

Once the feature vector databases are ready we can fire the desired query to retrieve the similar images from the database. To facilitate this, retrieval system has to perform the important task of applying the similarity measure so that distance between the query image and database image will be calculated and images having less distance will be retrieved in the final set. In this work we are using 6 similarity measures we named them L1 to L6, which includes Minkowski distance from order 1 to order 5(L1 to L5) and L6 is another distance i.e Correlation distance for the image retrieval. We have analyzed their performance using different evaluation parameters. These similarity measures are given in the following equations 5 and 6.

Minkowski Distance :	Cosine Correlation Distance :
$$Dist_{DQ} = \left(\sum_{I=1}^{n} \left| D_I - Q_I \right|^r \right)^{\frac{1}{r}} \quad (5)$$ Where r is a parameter, n is dimension and I is the component of Database and Query image feature vectors D and Q respectively.	$$\frac{(D(n)) \bullet (Q(n))}{\sqrt{\left[\left| D(n) \right|^2 \left| Q(n) \right|^2 \right]}} \quad (6)$$ Where D(n) and Q(n) are Database and Query feature Vectors resp.

Minkowski Distance: Here the parameter 'r' can be taken from 1 to ∞. We have used this distance with 'r' in the range from 1 to 5. When 'r' is =2 it is special case called Euclidean distance (L2).

Cosine Correlation Distance: This can be expressed in the terms of Cos θ

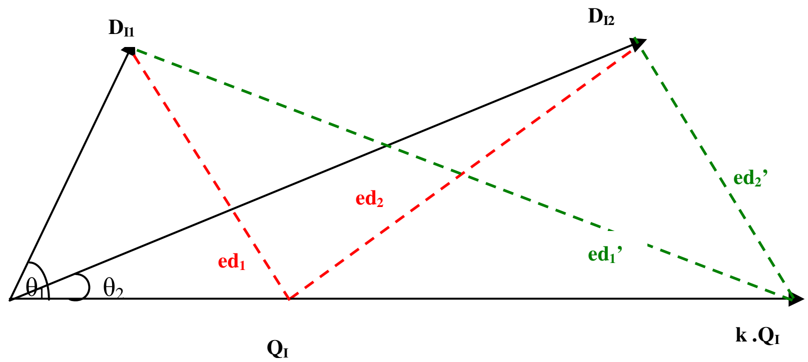

FIGURE 4 : Comparison of Euclidean and Cosine Correlation Distance

Observation: $ed_2 > ed_1$ But $ed_1' > ed_2'$

Correlation measures in general are invariant to scale transformations and tend to give the similarity measure for those feature vectors whose values are linearly related. In Figure 4. Cosine Correlation distance is compared with the Euclidean distance. We can clearly notice that Euclidean distance ed2 > ed1 between query image QI with two database image features DI1 and DI2 respectively for QI. At the same time we can see that θ1 > θ2 i.e distance L6 for DI1 and DI2 respectively for QI.

If we scaled the query feature vector by simply constant factor k it becomes k.QI ; now if we calculate the ED for DI1 and DI2 with query k.QI we got ed1' and ed2' now the relation they have is ed1' > ed2' which is exactly opposite to what we had for QI. But if we see the cosine correlation distance; it will not change even though we have scaled up the query feature vector to k.QI. It clearly states that Euclidean distance varies with variation in the scale of the feature vector but cosine correlation distance is invariant to this scale transformation. This property of correlation distance triggered us to make use this for our CBIR. Actually this has been rarely used for CBIR systems and here we found very good results for this similarity measure as compared to Euclidean distance and the higher orders of Minkowski distance.

2.4 Performance Evaluation

Results obtained here are interpreted in the terms of PRCP: Precision Recall Cross over Point. This parameter is designed using the conventional parameters precision and recall defined in equation 7 and 8.

According to this once the distance is calculated between the query image and database images, these distances are sorted in ascending order. According to PRCP logic we are selecting first 100 images from sorted distances and among these we have to count the images which are relevant to query; this is what called PRCP value for that query because we have total 100 images of each class in our database.

Precision: Precision is the fraction of the relevant images which has been retrieved (from all retrieved)

Recall: Recall is the fraction of the relevant images which has been retrieved (from all relevant):

$$\text{Precision} = \frac{\text{Number of Relevant Images Retreived}}{\text{Total Number of Images Retreieved}} \quad (7)$$

$$\text{Recall} = \frac{\text{Number of Relevant Images Retreived}}{\text{Total Number of Relevant Images in Database}} \quad (8)$$

Further performance of this system is evaluated using two more interesting parameters about which all CBIR users will always be curious, that are LSRR: Length of String to Retrieve all Relevant and Longest String: Longest continuous string of relevant images.

3. EXPERIMENTAL RESULTS AND DISCUSSIONS

In this work analysis is done to check the performance of the similarity measures for CBIR using bins approach. That is why the results presented are highlighting the comparative study for different similarity measures named as L1 to L6 as mentioned in above discussion.

3.1 Image Database and Query Images

Database used for the experiments is having 2000 BMP images which include 100 images from 20 different classes. The sample images from database are shown in Figure 5. We have randomly selected 10 images from each class to be given as query to the system to be tested. In

FIGURE 5 : 20 Sample Images from database of 2000 BMP images having 20 classes

all total 200 queries are executed for each feature vector database and for each similarity measure. We have already shown one sample query image in Figure 1. i.e. Kingfisher image for which the bins formation that is feature extraction process is explained thoroughly in section II part A and B.

3.2 Discussion With Respect to PRCP

As discussed above the feature vector databases containing feature vectors of 27 bins components for four absolute moments namely Mean, Standard deviation, Skewness and Kurtosis for Red, Green and Blue colors separately are tested with 200 query images for six similarity measures and the results obtained are given below in the following tables. Tables I to XII are showing the results obtained for parameter PRCP i.e. Precision Recall Cross over Point values for 10 queries from each class. Each entry in the table is representing the total retrieval of (out of 1000 outputs) relevant images in terms of PRCP for 10 queries of that particular class mentioned in the first left most column of all the tables. Last rows of all the tables represent the total PRCP retrieval out of 20,000 for 200 images. When we observe the individual entry in the tables that is total of 10 queries for many classes with respect to distances L1 and L6 we have found very good PRCP values for average of 10 queries in the range from 0.5 to 0.8 which is quite good achievement. We can say that precision and recall both are reached to good height which seems difficult in the field of CBIR for large size databases. Further we have planned to improve these results not limiting to average of 10 queries but towards average of 200 queries. To obtain this refinement what we did here is we have combined and reduced the results obtained for three colors separately to single results set of three colors together by applying the criterion explained below.

Criterion: The image will be retrieved in the final set if it is being retrieved in any one color results from R, G and B.

By applying this criterion to all results obtained for three colors, four moments mentioned in the tables from I to XII we have improved the system's performance to very good extent for average of 200 queries for moments namely Mean and Standard Deviation with similarity measures L1, L6, L2 and L3 in increasing order. Results obtained are shown in Chart 1. We can see in chart that the best average for 200 queries for PRCP values we could obtained is 0.5

TABLE 1: PRCP FOR RED MEAN FOR L1 TO L6

CLASS	L1	L2	L3	L4	L5	L6
Flower	388	321	264	225	198	357
Sunset	764	707	603	522	461	727
Mountain	144	116	117	112	110	114
Building	177	165	161	163	161	162
Bus	512	474	439	414	407	472
Diansour	251	202	171	152	145	192
Elephant	157	128	124	119	120	133
Barbie	517	483	474	438	432	504
Mickey	305	308	301	302	300	314
Horses	285	230	194	177	173	214
Kingfisher	300	258	235	223	215	268
Dove	207	194	196	185	178	187
Crow	177	169	183	183	185	106
Rainbowrose	643	618	596	585	575	638
Pyramids	186	141	114	121	121	135
Plates	238	199	176	163	142	197
Car	134	111	104	93	91	105
Trees	283	239	231	213	206	242
Ship	327	276	256	252	244	249
Waterfall	281	214	195	190	191	205
Total	6276	5553	5134	4832	4655	5521

TABLE 2: PRCP FOR GREEN MEAN FOR L1 TO L6

CLASS	L1	L2	L3	L4	L5	L6
Flower	258	214	182	173	165	239
Sunset	714	664	633	614	610	674
Mountain	147	127	121	124	126	124
Building	189	158	149	134	133	158
Bus	421	308	247	236	223	307
Dinosaur	223	189	168	163	160	200
Elephant	176	127	107	102	103	127
Barbie	537	503	486	478	468	463
Mickey	243	225	212	205	203	237
Horses	331	303	290	279	272	310
Kingfisher	350	314	286	282	286	321
Dove	199	188	179	170	166	190
Crow	147	136	120	117	115	110
Rainbowrose	652	613	590	563	555	647
Pyramids	172	138	114	110	106	132
Plates	240	215	198	169	156	210
Car	242	247	250	252	263	272
Trees	263	221	205	185	167	227
Ship	302	289	285	270	266	294
Waterfall	226	182	175	162	157	191
Total	6032	5361	4997	4788	4700	5433

CHART 1:. Results using Criterion to combine the R, G B color results for L1 to

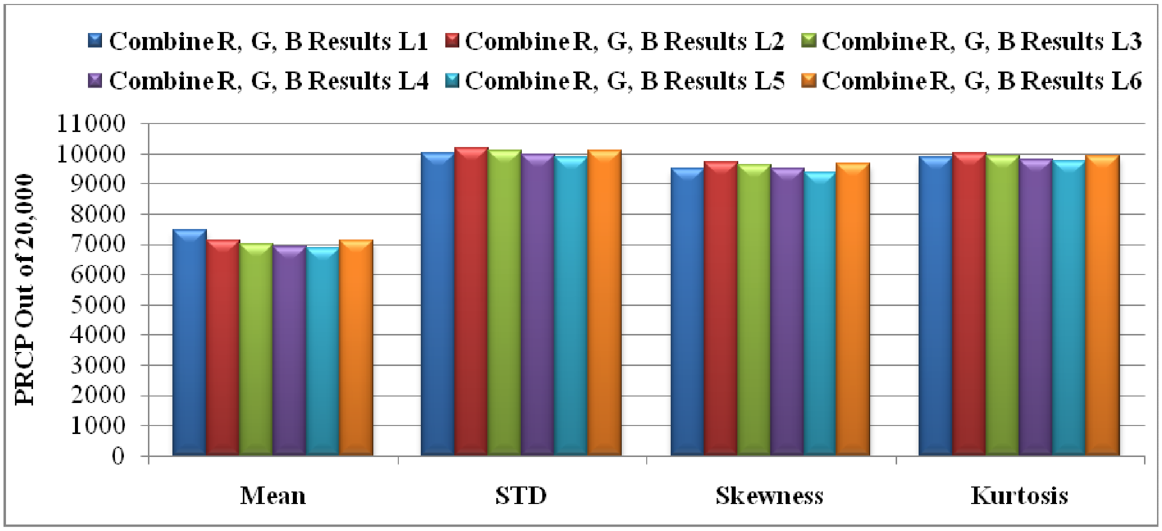

L6.

TABLE 3: PRCP FOR BLUE MEAN FOR L1 TO L6

CLASS	L1	L2	L3	L4	L5	L6
Flower	313	340	315	286	268	374
Sunset	542	479	474	463	455	445
Mountain	173	156	147	141	142	160
Building	170	136	114	109	100	139
Bus	433	355	346	334	327	357
Diansour	233	188	167	144	152	180
Elephant	193	176	162	145	142	183
Barbie	476	395	411	380	375	416
Mickey	217	189	173	162	161	196
Horses	297	230	192	185	183	236
Kingfisher	337	332	340	344	351	340
Dove	201	178	140	117	114	195
Crow	127	96	84	72	67	96
Rainbowrose	642	635	627	621	611	662
Pyramids	165	113	93	90	88	106
Plates	234	204	180	169	161	189
Car	162	146	138	131	132	131
Trees	251	195	165	154	153	200
Ship	307	245	203	191	180	246
Waterfall	252	176	147	135	138	187
Total	5725	4964	4618	4373	4300	5038

TABLE 4 : PRCP FOR RED STD FOR L1 TO L6

CLASS	L1	L2	L3	L4	L5	L6
Flower	312	296	279	257	243	298
Sunset	719	681	648	619	600	726
Mountain	206	208	190	172	167	199
Building	278	262	249	235	228	257
Bus	508	481	455	430	417	484
Diansour	409	430	416	416	406	366
Elephant	286	311	320	336	342	304
Barbie	485	433	386	337	320	426
Mickey	254	244	241	230	223	242
Horses	513	509	479	454	437	518
Kingfisher	417	429	420	404	388	441
Dove	330	309	275	251	237	306
Crow	201	194	188	184	184	127
Rainbowrose	501	507	498	469	448	588
Pyramids	285	281	266	258	248	222
Plates	323	300	280	267	255	329
Car	211	204	180	176	173	244
Trees	310	300	294	290	285	268
Ship	389	354	332	312	306	394
Waterfall	422	430	434	425	425	442
Total	7359	7163	6830	6522	6332	7181

4. PERFORMANCE EVALUATION USING LONGEST STRING AND LSRR PARAMETERS

Along with the conventional parameters precision and recall used for CBIR we have evaluated the system performance using two additional parameters namely Longest String and LSRR. As discussed in section 2.4, CBIR users will always have curiosity to check what will be the maximum continuous string of relevant images in the retrieval set which can be obtained using the parameter longest string. LSRR gives the performance of the system in terms of the maximum length of the sorted distances of all database images to be traversed to collect all relevant images of the query class.

4.1 Longest String

This parameter is plotted through various charts. As we have 12 different feature vector databases prepared for 4 moments for each of the three colors separately. We have calculated the longest string for all the 12 database results, but the plots for longest string are showing the maximum longest string obtained for each class for distances L1 to L6 irrespective of the three colors and this way we have obtained total 4 sets of results plotted in charts 2, 3, 4 and 5 for first four moments respectively. Among these few classes like Sunset, Rainbow rose, Barbie, Horses and Pyramids are giving very good results that more than 60 as maximum longest string of relevant images we could retrieve. In all the resultant bar of all graphs we can notice that L1 and L6 are reaching to good height of similarity retrieval.

TABLE 5 : PRCP FOR GREEN STANDARD DEV.

CLASS	L1	L2	L3	L4	L5	L6
Flower	320	352	332	319	296	376
Sunset	802	794	771	746	729	789
Mountain	243	249	236	225	223	238
Building	310	312	306	303	297	283
Bus	463	430	392	367	346	465
Diansour	359	358	347	338	328	304
Elephant	321	335	333	334	334	328
Barbie	461	416	401	395	385	430
Mickey	239	238	217	210	210	241
Horses	523	470	412	374	352	473
Kingfisher	368	389	363	353	348	383
Dove	355	307	270	243	238	315
Crow	238	211	192	192	187	120
Rainbowrose	647	652	624	590	577	708
Pyramids	351	350	334	323	319	174
Plates	345	345	330	317	311	370
Car	323	355	354	343	339	389
Trees	295	274	269	265	258	270
Ship	378	342	316	306	304	377
Waterfall	421	423	410	403	407	412
Total	7762	7602	7209	6946	6788	7445

TABLE 6 : PRCP FOR BLUE STANDARD DEV.

CLASS	L1	L2	L3	L4	L5	L6
Flower	315	324	319	318	315	325
Sunset	696	593	529	483	462	630
Mountain	210	204	217	212	212	209
Building	224	214	194	191	183	196
Bus	480	484	474	439	422	531
Diansour	318	298	278	273	271	261
Elephant	228	252	257	256	259	245
Barbie	454	363	319	284	264	381
Mickey	222	213	199	196	190	229
Horses	453	446	425	404	403	445
Kingfisher	322	336	333	321	318	333
Dove	352	334	300	280	262	338
Crow	208	165	160	158	152	109
Rainbowrose	615	619	599	587	558	687
Pyramids	242	238	232	228	226	196
Plates	263	261	255	251	246	290
Car	227	218	211	195	187	250
Trees	253	228	215	200	191	227
Ship	414	402	387	375	367	435
Waterfall	273	258	247	246	239	260
Total	6769	6450	6150	5897	5727	6577

4.2 LSRR

Similar to Longest String, the parameter LSRR is also used to evaluate the performance of 12 feature vector databases. As said earlier it gives the maximum length we need to travel in the string of distances sorted in ascending order to collect all images from database which are relevant to query image or say of query class. According to this logic of LSRR ; the value of LSRR should be as low as possible so that with minimum traversal length and with less time we can recall all the images from database. Results obtained for this parameter are the minimum values in terms of percentage of LSRR are calculated for all 12 feature vector databases for 200 query images with respect to all six similarity measures. The chart 6 is showing the results as best of LSRR that is minimum LSRR for each class of image for all distance measures L1 to L6 irrespective of three colors and four moments.

CHART 2: Max. In Results of Longest string of Mean parameter into 27 Bins

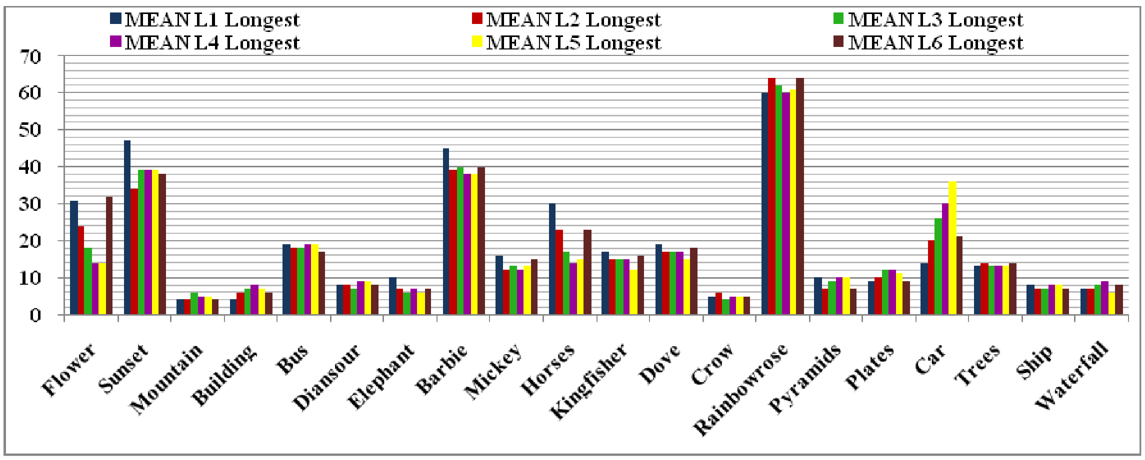

TABLE 7 : PRCP FOR RED SKEWNESS

CLASS	L1	L2	L3	L4	L5	L6
Flower	268	221	197	193	183	232
Sunset	646	578	524	495	482	635
Mountain	209	200	185	177	169	200
Building	223	211	199	182	176	214
Bus	422	411	391	380	369	429
Diansour	347	334	317	304	293	283
Elephant	246	271	280	281	277	237
Barbie	482	406	350	312	290	393
Mickey	245	249	241	237	226	229
Horses	399	389	350	313	303	391
Kingfisher	365	376	348	321	304	390
Dove	335	350	354	349	343	384
Crow	167	142	139	139	141	123
Rainbowrose	359	394	391	382	374	489
Pyramids	225	190	174	168	162	198
Plates	267	232	196	178	163	247
Car	155	161	157	152	148	225
Trees	296	279	260	248	247	225
Ship	342	297	268	256	249	311
Waterfall	362	352	332	319	309	263
Total	6360	6043	5653	5386	5208	6098

TABLE 8 : PRCP FOR GREEN SKEWNESS

CLASS	L1	L2	L3	L4	L5	L6
Flower	375	361	319	291	275	379
Sunset	674	617	563	530	506	679
Mountain	216	203	191	184	186	205
Building	252	224	214	207	212	203
Bus	441	418	378	349	342	451
Diansour	293	257	230	220	210	200
Elephant	222	227	219	210	206	204
Barbie	459	450	451	450	446	436
Mickey	234	237	226	213	208	233
Horses	383	335	294	271	248	380
Kingfisher	327	356	354	354	343	355
Dove	349	336	316	305	300	370
Crow	181	161	146	143	137	134
Rainbowrose	508	540	519	500	481	577
Pyramids	282	298	284	273	268	153
Plates	237	236	228	218	211	246
Car	276	363	374	377	367	404
Trees	216	180	173	174	170	192
Ship	316	281	267	257	249	292
Waterfall	321	292	267	250	248	279
Total	6562	6372	6013	5776	5613	6372

CHART 3: Max. In Results of Longest String of Standard Deviation parameter 27 Bins

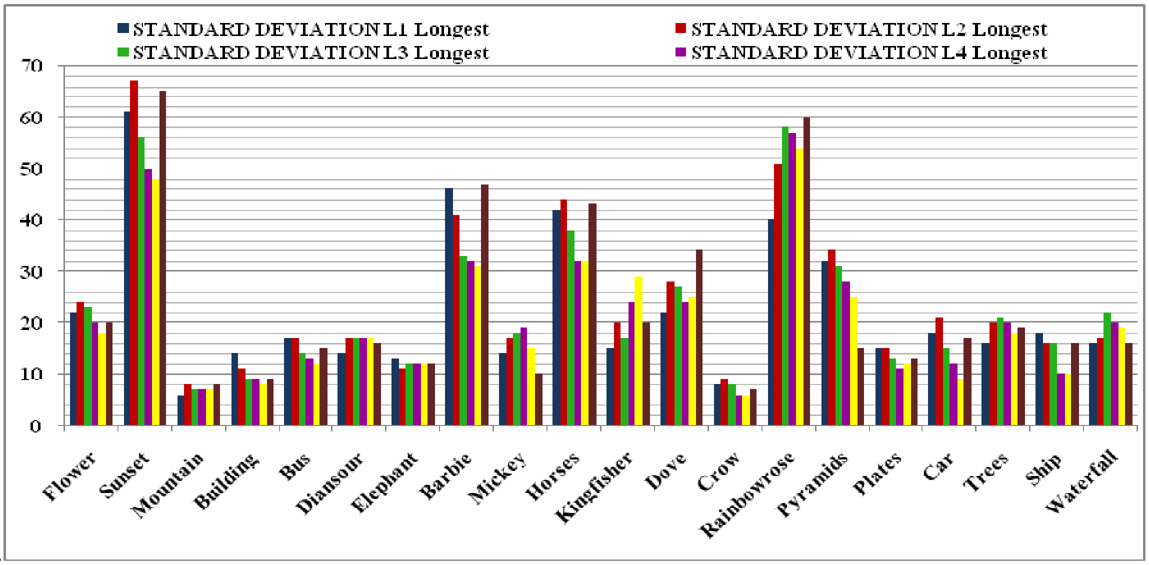

TABLE 9: PRCP FOR BLUE SKEWNESS

CLASS	L1	L2	L3	L4	L5	L6
Flower	335	331	322	314	302	342
Sunset	666	607	540	513	481	576
Mountain	205	208	201	195	191	209
Building	179	174	164	153	145	168
Bus	416	433	416	386	370	497
Diansour	290	247	231	226	222	244
Elephant	168	169	161	162	162	173
Barbie	458	419	387	372	341	413
Mickey	219	215	211	208	204	218
Horses	434	438	417	404	394	461
Kingfisher	247	262	258	255	250	253
Dove	385	346	333	317	314	399
Crow	177	162	147	153	149	118
Rainbowrose	490	514	519	517	497	575
Pyramids	204	195	184	174	169	194
Plates	249	241	230	218	210	262
Car	169	192	187	185	181	225
Trees	252	218	199	188	184	200
Ship	331	313	284	272	264	317
Waterfall	236	219	208	208	200	204
Total	6110	5903	5599	5420	5230	6048

TABLE 10: PRCP FOR RED KURTOSIS

CLASS	L1	L2	L3	L4	L5	L6
Flower	337	302	273	254	243	326
Sunset	340	695	655	624	610	734
Mountain	727	210	196	193	188	202
Building	217	240	226	220	218	257
Bus	274	493	485	468	459	500
Diansour	524	354	342	325	318	283
Elephant	349	343	355	361	367	333
Barbie	311	447	400	366	342	438
Mickey	488	255	240	236	227	250
Horses	260	486	461	432	416	511
Kingfisher	496	444	430	410	393	440
Dove	439	362	354	351	345	402
Crow	355	164	161	155	147	124
Rainbowrose	167	534	522	504	488	599
Pyramids	516	269	256	250	240	222
Plates	280	300	276	267	259	320
Car	315	190	179	176	174	242
Trees	206	287	282	269	269	260
Ship	309	363	334	322	316	389
Waterfall	405	434	436	430	422	420
Total	7315	7172	6863	6613	6441	7252

CHART 4: Max. In Results of Longest String of Skewness parameter 27 Bins

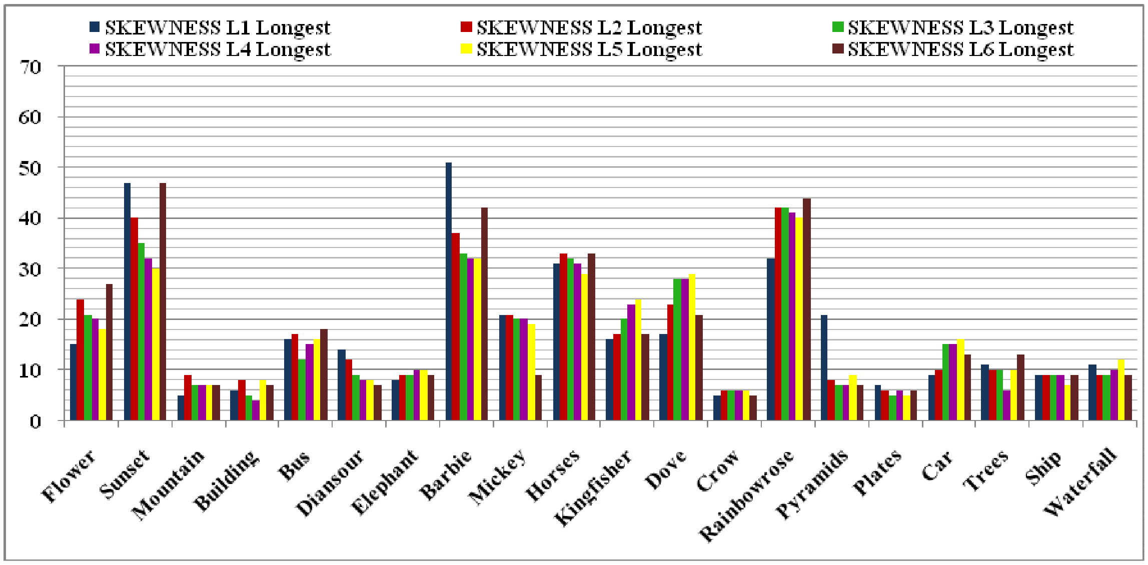

TABLE 11 : PRCP FOR GREEN KURTOSIS

	L1	L2	L3	L4	L5	L6
Flower	393	412	386	369	350	423
Sunset	801	788	761	735	717	803
Mountain	263	256	239	240	232	240
Building	316	295	289	281	267	274
Bus	533	478	428	411	384	503
Diansour	308	297	287	275	271	245
Elephant	321	323	329	328	329	313
Barbie	452	446	440	440	444	440
Mickey	254	246	241	220	210	238
Horses	512	441	377	343	326	454
Kingfisher	388	415	407	398	390	417
Dove	374	350	323	319	309	380
Crow	197	185	177	162	155	125
Rainbowrose	677	679	655	631	606	713
Pyramids	335	340	317	309	303	168
Plates	338	335	315	313	313	353
Car	327	363	357	358	356	398
Trees	279	249	245	240	231	251
Ship	395	344	320	306	302	368
Waterfall	413	406	390	385	382	397
Total	7876	7648	7283	7063	6877	7503

TABLE 12 : PRCP FOR BLUE KURTOSIS

	L1	L2	L3	L4	L5	L6
Flower	346	347	345	338	330	352
Sunset	760	688	604	566	541	674
Mountain	200	205	205	214	214	209
Building	214	208	196	189	177	205
Bus	487	493	459	436	420	530
Diansour	303	276	270	257	254	252
Elephant	211	224	231	230	230	234
Barbie	460	414	374	354	346	407
Mickey	231	222	218	213	212	231
Horses	469	454	449	434	422	459
Kingfisher	327	354	348	334	339	337
Dove	400	367	341	325	323	409
Crow	160	145	132	128	128	105
Rainbowrose	630	635	621	608	584	691
Pyramids	240	244	250	251	241	218
Plates	267	262	259	255	253	284
Car	214	211	197	187	183	235
Trees	246	216	196	185	179	204
Ship	407	393	380	370	360	408
Waterfall	276	249	243	244	245	253
Total	6848	6607	6318	6118	5981	6697

CHART 5 : Max. In Results of Longest String of Kurtosis Parameter _27 Bins

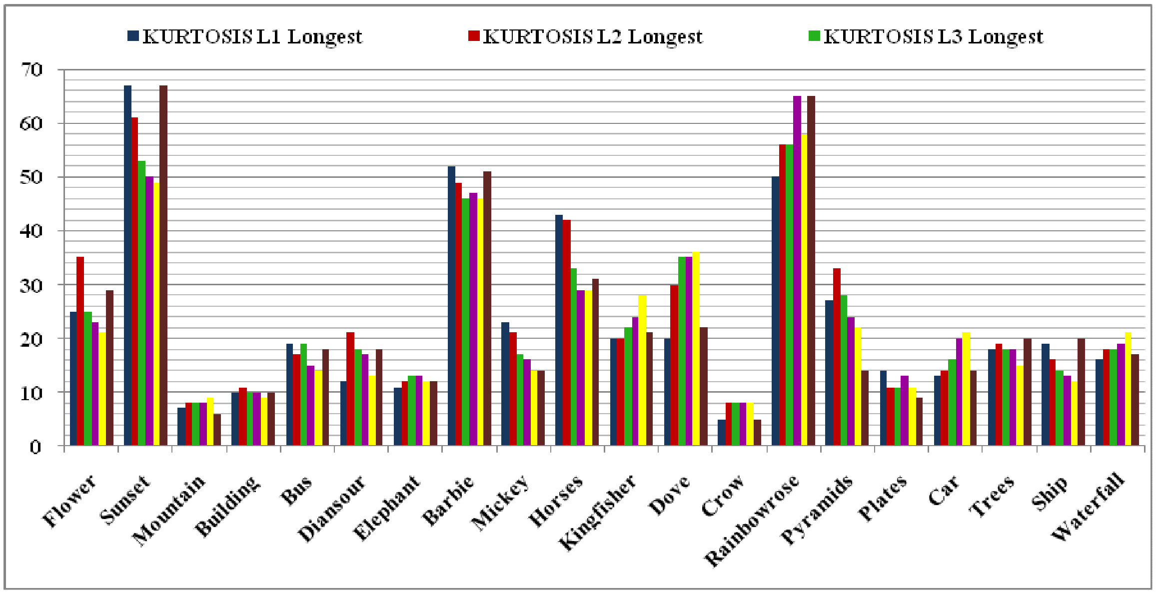

CHART 6. Min. In Results of LSRR for L1 to L6 Irrespective of Color and Moment

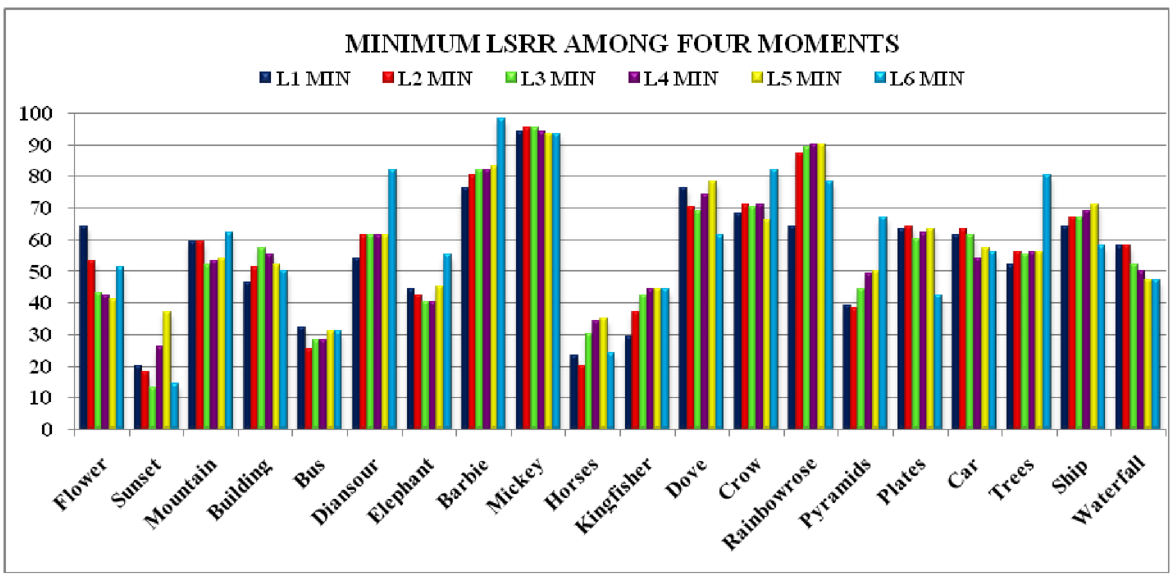

In above chart we can observe that many classes are performing well means minimum traversal is giving 100% recall for them the classes giving best results are sunset, bus, horses, kingfisher and pyramids etc. among these best is Sunset class where 14 %, traversal of 2000 images only will give 100 % recall for sunset query for L6, 20% for L1 distance measure.

We have shown first few images from the PRCP result obtained for Kingfisher query image in Figure 6. This is obtained for feature vector Green Kurtosis with the L1 distance measures. We retrieved total 65 images as PRCP(from first 100) for this query.

Query Image

Retreived Images…

FIGURE 6 : Query Image and first 46 images retreived out of 65

CONCLUSION

The ‘Bins Approach’ explained in this paper is new and simple in terms of computational complexity for feature extraction. It is based on histogram partitioning of three color planes. As histogram is partitioned into 3 parts, we could form 27 bins out of it. These bins are directed to extract the features of images in the form of four statistical moments namely Mean, Standard Deviation, Skewness and Kurtosis.

Similarity measures used to facilitate the comparison of database and query images we have used two similarity measures that are Minkowski distance and Cosine correlation distance. We have used multiple variations of Minkowski distance from order 1 to order 5 with nomenclature L1 to L5 and L6 is used for cosine correlation distance. Among these six distances L1 and L6 are giving best performance as compared to other increasing orders of Minkowski distance. Here we have seen that performance goes on decreasing with increase in Minkowski order parameter 'r' given in equation 5.

Conventional CBIR systems are mostly designed with Euclidean distance. We have shown the effective use of other two similarity measures 'Absolute distance' and 'Cosine correlation distance'. The work presented in this paper has proved that AD and CD are giving far better performance as compared to the commonly adopted conventional similarity measure Euclidean distance. In all tables having PRCP results we have highlighted first two best results and after counting them and comparing we found that AD and CD are better in maximum cases as compared to ED.

Comparative study of types of feature vectors based on moments, even moments are performing better as compared to odd moments i.e. standard deviation and kurtosis are better than mean and skewness.

Observation of all performance evaluation parameters delineates that the best value obtained for PRCP is 0.8 for average of 10 queries for many out of the 20 classes. Whereas combining the R, G, B color results using special criterion; the best value of PRCP works out to 0.5 for average of 200 queries which is the most desirable performance for any CBIR. The maximum longest string of relevant images obtained is for class rainbow rose and sunset; the value is around 70 (out of 100) for L1 and L6 distance measure as shown in charts 3 and 5 for even moments. The minimum length traversed to retrieve all the relevant images from database i.e LSRR's best value is 14% for L6 and 20% for L1 for class sunset.

We have also worked with 8 bins and 64 bins by dividing the equalized histogram in 2 and 4 parts respectively. However the best results are obtained for 27 bins which are presented here.

REFERENCES

[1] Yong Rui and Thomas S. Huang , "Image Retrieval: Current Techniques, Promising Directions, and Open Issues" Journal of Visual Communication and Image Representation 10, 39–62 (1999).

[2] Dr. H.B. Kekre, Mr. Dhirendra Mishra, Mr. Anirudh Kariwala , "Survey Of Cbir Techniques And Semantics". International Journal of Engineering Science and Technology (IJEST), Vol. 3 No. 5 May 2011.

[3] Raimondo Schettini, G. Ciocca, S. Zuffi, "A Survey Of Methods For Color Image Indexing And Retreival In Image Databases". www.intelligence.tuc.gr/~petrakis/courses/.../papers/color-survey.pdf

[4] Sameer Antania, Rangachar Kasturia; , Ramesh Jainb "A surveyon the use of pattern recognition methods for abstraction, indexing and retrieval of images and video" Pattern Recognition 35 (2002) 945–965.

[5] Hualu Wang, Ajay Divakaran, Anthony Vetro, Shih-Fu Chang, and Huifang Sun "Survey of compressed-domain features used in audio-visual indexing and analysis" 2003 Elsevier Science (USA). All rights reserved.doi:10.1016/S1047-3203(03)00019-1.

[6] S. Nandagopalan, Dr. B. S. Adiga, and N. Deepak, " A Universal Model for Content-Based Image Retrieval" World Academy of Science, Engineering and Technology 46 2008.

[7] C. W.Ngo, T. C. Pong, R.T. Chin. "Exploiting image indexing techniques in DCT domain" IAPR International Workshop on multimedia Media Information Analysis and Retrieval.

[8] Elif Albuz, Erturk Kocalar, and Ashfaq A. Khokhar, " Scalable Color Image Indexing And Retrieval Using Vector Wavelets" IEEE Transactions on Knowledge and Data Engineering, Volume 13 Issue 5, September 200.

[9] Mann-Jung HsiaoYo-Ping HuangTe-Wei Chiang, "A Region-Based Image Retrieval Approach Using Block DCT" 0-7695-2882-1/07 $25.00 ©2007 IEEE.

[10] Wu Xi, Zhu Tong, "Image Retrieval based on Multi-wavelet Transform" 978-0-7695-3119-9/08 $25.00 © 2008 IEEE, 2008 Congress on Image and Signal Processing.

[11] H. B. Kekre , Kavita Sonawane, Query Based Image Retrieval Using kekre's, DCT and Hybrid wavelet Transform Over 1st and 2nd Moment, International Journal of Computer Applications (0975 – 8887), Volume 32– No.4, October 2011.

[12] H. B. Kekre, Kavita Sonawane, Retrieval of Images Using DCT and DCT Wavelet Over Image Blocks. (IJACSA) International Journal of Advanced Computer Science and Applications, Vol. 2, No. 10, 2011.

[13] Arnold W.M. Smeulders, Senior Member, IEEE, Marcel Worring, Simone Santini, Member, IEEE, Amarnath Gupta, Member, IEEE, and Ramesh Jain, Fellow, IEEE , " Content-Based Image Retrieval at the End of the Early Years".

[14] Zur Erlangung des Doktorgradesder Fakult, Angewandte Wissenschaften "Feature Histograms for Content-Based Image Retrieval"2002

[15] Young Deok Chun, Sang Yong Seo, and Nam Chul Kim ,"Image Retrieval Using BDIP and BVLC Moments", IEEE Transactions On Circuits And Systems For Video Technology, Vol. 13, No. 9, September 2003.

[16] Dr. H.B.Kekre, Dr. Sudeep D. Thepade, Shrikant P. Sanas, Sowmya Iyer , "Shape Content Based Image Retrieval using LBG VectorQuantization." (IJCSIS) International Journal of Computer Science and Information Security,Vol. 9, No. 12, December 2011.

[17] H.B.Kekre, Sudeep D. Thepade, Tanuja K. Sarode, Shrikant P. Sanas "Image Retrieval Using Texture Features Extracted Using Lbg, Kpe, Kfcg, Kmcg, Kevr With Assorted Color Spaces", International Journal of Advances in Engineering & Technology, Jan 2012.©IJAET ISSN: 2231-1963 520 Vol. 2, Issue 1, pp. 520-531.

[18] Dr. H.B.Kekre , Kavita Sonawane, Bins Approach To Image Retrieval Using Statistical Parameters Based On Histogram Partitioning Of R, G, B Planes, Jan 2012. ©IJAET ISSN: 2231-1963.

[19] Image Retrieval Using BDIP and BVLC Moments, Young Deok Chun, Sang Yong Seo, and Nam Chul Kim, IEEE Transactions On Circuits And Systems For Video Technology, Vol. 13, No. 9, September 2003.

[20] H. B. Kekre , Kavita Sonawane, "Feature Extraction in Bins Using Global and Local thresholding of Images for CBIR" International Journal Of Computer Applications In Applications In Engineering, Technology And Sciences, ISSN: 0974-3596, October '09 – March '10, Volume 2 : Issue 2

[21] Guang Yang, Yingyuan Xiao, "A Robust Similarity Measure Method in CBIR System" 978-0-7695-3119-9/08 $25.00 © 2008 IEEE, 2008 Congress on Image and Signal Processing.

[22] Zhi-Hua Zhou Hong-Bin Dai, "Query-Sensitive Similarity Measure for Content-Based Image Retrieval"ICDM, 06, Proceeding's of sixth International Conference on data Mining. IEEE Comp. Society, Washington, DC, USA 2006.

[23] Ellen Spertus, Mehran Sahami, Orkut Buyukkokten, "Evaluating Similarity Measures:A LargeScale Study in the Orkut Social network" Copyright 2005ACM.The definitive version was published in KDD '05, August 2124, 2005http://doi.acm.org/10.1145/1081870.1081956.

[24] Simone Santini, Member, IEEE, and Ramesh Jain, Fellow, IEEE, "Similarity Measures" IEEETransactions On Pattern Analysis And Machine Intelligence, Vol. 21, No. 9, September 1999.

[25] John P., Van De Geer, "Some Aspects of Minkowski distance", Department of data theory, Leiden University. RR-95-03.

[26] Dengsheng Zhang and Guojun Lu "Evaluation Of Similarity Measurement For Image Retrieval" www. Gscit.monash.edu.au/~dengs/resource/papers/icnnsp03.pdf.

[27] Gang Qian, Shamik Sural, Yuelong Gu† Sakti Pramanik, "Similarity between Euclidean and cosine angle distance fornearest neighbor queries", SAC'04, March 14-17, 2004, Nicosia, Cyprus Copyright 2004 ACM 1-58113-812-1/03/04.

[28] Sang-Hyun Park, Hyung Jin Sung, "Correlation Based Image Registration for Pressure Sensitive Paint", flow.kaist.ac.kr/upload/paper/2004/SY2004.pdf .

[29] Julia Vogela, Bernt Schiele, "Performance evaluation and optimization for content-based image retrieval", 0031-3203/$30.00 _ 2005 Pattern Recognition Society. Published by Elsevier Ltd. All rights reserved. doi:10.1016/j.patcog.2005.10.024

[30] Stéphane Marchand-Maillet, "Performance Evaluation in Content-based Image Retrieval:The Benchathlon Network",

[31] Thomas Deselaers, Daniel Keysers, and Hermann Ney , "Classification Error Rate for Quantitative Evaluation of Content-based Image Retrieval Systems" http://www.cs.washington.edu/research/imagedatabase/groundtruth/, and http://www-i6.informatik.rwthaachen.de/˜deselaers/uwdb

[32] Dr. H. B. Kekre, Dhirendra Mishra "Image Retrieval using DST and DST Wavelet Sectorization", (IJACSA) International Journal of Advanced Computer Science and Applications, Vol. 2, No. 6, 2011.

[33] Dr. H. B. Kekre, Kavita Sonawane," Image Retrieval Using Histogram Based Bins of Pixel Counts and Average of Intensities", (IJCSIS) International Journal of Computer Science and Information Security, Vol. 10, No.1, 2012

INSTRUCTIONS TO CONTRIBUTORS

The *International Journal of Image Processing (IJIP)* aims to be an effective forum for interchange of high quality theoretical and applied research in the Image Processing domain from basic research to application development. It emphasizes on efficient and effective image technologies, and provides a central forum for a deeper understanding in the discipline by encouraging the quantitative comparison and performance evaluation of the emerging components of image processing.

We welcome scientists, researchers, engineers and vendors from different disciplines to exchange ideas, identify problems, investigate relevant issues, share common interests, explore new approaches, and initiate possible collaborative research and system development.

To build its International reputation, we are disseminating the publication information through Google Books, Google Scholar, Directory of Open Access Journals (DOAJ), Open J Gate, ScientificCommons, Docstoc and many more. Our International Editors are working on establishing ISI listing and a good impact factor for IJIP.

The initial efforts helped to shape the editorial policy and to sharpen the focus of the journal. Starting with volume 6, 2012, IJIP appears in more focused issues. Besides normal publications, IJIP intends to organize special issues on more focused topics. Each special issue will have a designated editor (editors) – either member of the editorial board or another recognized specialist in the respective field.

We are open to contributions, proposals for any topic as well as for editors and reviewers. We understand that it is through the effort of volunteers that CSC Journals continues to grow and flourish.

LIST OF TOPICS
The realm of International Journal of Image Processing (IJIP) extends, but not limited, to the following:

- Architecture of imaging and vision systems
- Autonomous vehicles
- Character and handwritten text recognition
- Chemical and spectral sensitization
- Chemistry of photosensitive materials
- Coating technologies
- Coding and transmission
- Cognitive aspects of image understanding
- Color imaging
- Communication of visual data
- Data fusion from multiple sensor inputs
- Display and printing
- Document image understanding
- Generation and display
- Holography
- Image analysis and interpretation
- Image capturing, databases
- Image generation, manipulation, permanence
- Image processing applications
- Image processing: coding analysis and recognition
- Image representation, sensing
- Imaging systems and image scanning
- Implementation and architectures
- Latent image
- Materials for electro-photography
- Network architecture for real-time video transport
- New visual services over ATM/packet network
- Non-impact printing technologies
- Object modeling and knowledge acquisition
- Photoconductors
- Photographic emulsions
- Photopolymers
- Prepress and printing technologies
- Protocols for packet video
- Remote image sensing
- Retrieval and multimedia

- Storage and transmission
- Video coding algorithms and technologies for ATM/p

CALL FOR PAPERS

Volume: 6 - **Issue: 5** - October 2012

i. Paper Submission: July 31, 2012 **ii. Author Notification:** September 15, 2012

iii. Issue Publication: October 2012

CONTACT INFORMATION

Computer Science Journals Sdn BhD
B-5-8 Plaza Mont Kiara, Mont Kiara
50480, Kuala Lumpur, MALAYSIA
Phone: 006 03 6207 1607
006 03 2782 6991

Fax: 006 03 6207 1697

Email: cscpress@cscjournals.org

CSC PUBLISHERS © 2012
COMPUTER SCIENCE JOURNALS SDN BHD
M-3-19, PLAZA DAMAS
SRI HARTAMAS
50480, KUALA LUMPUR
MALAYSIA

PHONE: 006 03 6207 1607
006 03 2782 6991

FAX: 006 03 6207 1697
EMAIL: cscpress@cscjournals.org